



BIRZEIT UNIVERSITY

BIRZEIT UNIVERSITY

FACULTY OF ENGINEERING & TECHNOLOGY

DEPARTMENT OF ELECTRICAL & COMPUTER ENGINEERING

"SKIN DISEASE DETECTION USING DEEP LEARNING AND IMAGE PROCESSING"

Prepared By:

Rahaf Naser 1201319

Hala Mosafer 1202223

Rania Rimawi 1201179

Supervised By:

Dr. Nofal Nofal

(ENCS5300-Section 46)

A Graduation Project submitted to the Department of Electrical and Computer
Engineering in partial fulfillment of the requirements for the degree of B.Sc. in Computer
Engineering

BIRZEIT

July | 2025

Abstract

Skin diseases are among the most prevalent health conditions worldwide, affecting millions of people across all age groups. Early and accurate detection of these diseases is crucial for timely treatment and to prevent complications or progression to more severe stages. However, manual diagnosis by dermatologists can be time-consuming, error-prone, and difficult to access in remote or underserved areas. In this project, we present a deep learning-based automated system for the classification of ten different skin diseases using dermoscopic images. The system is built using Python and PyTorch and leverages four different convolutional neural network (CNN) architectures—namely, a custom CNN, ResNet50, DenseNet121, and MobileNetV2. These models were trained and evaluated on a large, publicly available dataset sourced from Kaggle, which contains over 25,000 labeled clinical images spanning ten disease classes such as melanoma, eczema, and basal cell carcinoma.

All models were trained using advanced preprocessing techniques including resizing, normalization, data augmentation, and class balancing via weighted loss functions to improve generalization and address data imbalance. The dataset was split using a stratified approach to ensure representative distribution across training, validation, and test sets. After thorough experimentation and validation, the **MobileNetV2 model** achieved the highest classification accuracy and overall performance. MobileNetV2 not only outperformed the deeper DenseNet and ResNet architectures in accuracy but also proved to be highly efficient, making it suitable for real-time applications and mobile deployment.

To make the system accessible to non-technical users, the best-performing model was exported as a PyTorch module and integrated into a **Flask-based web application**. The web interface allows users to upload or capture an image of a skin lesion and instantly receive predictions, including the most probable disease class along with the associated confidence score. The interface is user-friendly and designed to assist in rapid screening or pre-diagnosis. This end-to-end solution showcases the powerful synergy between deep learning and web technology, offering a scalable and accessible tool for early skin disease detection. Overall, this project highlights the effectiveness of transfer learning, model optimization, and deployment strategies in solving real-world healthcare problems using artificial intelligence.

المستخلص

تُعد الأمراض الجلدية من أكثر الحالات الصحية انتشاراً على مستوى العالم، حيث تؤثر على ملايين الأشخاص من مختلف الأعمار. ويُعتبر الكشف المبكر والدقيق عن هذه الأمراض أمراً بالغ الأهمية لتمكين العلاج الفوري والحد من تفاقم الأعراض أو تطورها إلى مراحل أكثر خطورة. إلا أن عملية التشخيص اليدوي من قبل أطباء الجلد قد تكون مستغرقة للوقت، وعُرضة للخطأ، كما قد يصعب الوصول إليها في المناطق النائية أو ذات الموارد المحدودة. يهدف هذا المشروع إلى تطوير نظام آلي يعتمد على تقنيات التعلم العميق لتصنيف عشرة أنواع مختلفة من الأمراض الجلدية باستخدام صور جلدية سريرية. تم بناء النظام باستخدام لغة PyTorch ومكتبة Python ، مع تدريب أربعة نماذج مختلفة من الشبكات العصبية الالتفافية(CNN) ، وهي: نموذج CNN مخصص، ResNet50، DenseNet121، وMobileNetV2. وقد تم تدريب هذه النماذج على مجموعة بيانات موسومة ومتاحة عبر منصة Kaggle ، تحتوي على أكثر من 25,000 صورة جلدية موزعة على عشر فئات مرضية تشمل الميلانوما، والأكزيما، وسرطان الخلايا القاعدية.

تم تنفيذ عمليات معالجة متقدمة للصور شملت تغيير الأبعاد، وتوحيد القيم اللونية، وتطبيق تقنيات التحسين (augmentation) لزيادة تنوع البيانات، بالإضافة إلى موازنة الفئات من خلال استخدام دالة خسارة تعتمد على الأوزان. تم تقسيم البيانات بطريقة متوازنة (stratified split) لضمان تمثيل عادل لكل الفئات فيمجموعات التدريب والتحقق والاختبار. بعد إجراء تجارب موسعة، أظهر نموذج MobileNetV2 أفضل أداء من حيث الدقة والسرعة، متفوقاً على النماذج الأخرى بما في ذلك DenseNet121 وResNet50، مما يجعله مناسباً للاستخدام في الوقت الفعلي وحتى في التطبيقات المحمولة.

ولتحقيق سهولة الاستخدام، تم تصدير النموذج الأفضل إلى وحدة PyTorch وربطه بواجهة Web بنية باستخدام إطار العمل Flask. تتيح الواجهة للمستخدمين رفع صورة لافة جلدية أو التقاطها مباشرة من الكاميرا، ليتم تحليلها وإعطاء التنبؤ الأعلى احتمالاً مع درجة الثقة. تم تصميم التطبيق ليكون بسيطاً وسهل الاستخدام، ما يجعله أداة مناسبة للمساعدة في التشخيص المبكر أو الفحص السريع. يُبرز هذا المشروع الإمكانيات الكبيرة التي تتيحها تقنيات الذكاء الاصطناعي في المجال الطبي، كما يثبت أن الدمج بين التعلم العميق وتطوير التطبيقات يمكن أن ينتج عنه أدوات فعالة وقابلة للنشر تخدم المجتمع وتدعم رعاية صحية أفضل.

Contents

<i>Abstract</i>	I
المستخلص	II
List of Figures	V
List of Tables	VII
List of Abbreviations	VIII
Introduction	1
1.1 Background	1
1.2 AI and Deep Learning in Medical Imaging	2
1.3 Motivation.....	2
1.4 Problem Statement.....	3
1.5 Objectives.....	3
1.6 Scope of the Project.....	4
Literature Review	5
2.1 Skin Disease Detection in Medical Research	5
2.2 Deep Learning in Medical Image Analysis	5
2.3 Models Comparison	6
2.4 Gaps in Existing Research.....	8
2.5 Contribution of This Project.....	9
Skin Disease Detection and Classification	11
3.1 Skin Disease Definition and Classification.....	11
3.2 Methods Used to Detect Skin Diseases	13
3.3 Risk Factors.....	15
Related Works	17
4.1 Skin Disease Classification	17
4.1.1 Classification Models on Dermoscopic and Clinical Images	17
4.1.2 Efficient Mobile Architectures for Skin Disease Classification	18
3.2 Key Findings from Existing Research.....	20
Methodology and Evaluation Calculations	21
5.1 Dataset.....	21
5.2 Deep Learning Models.....	25

5.3 Training	27
5.4 MobileNetV2 Architecture Advantages.....	33
5.5 Multi-Class Classification Strategy	34
5.6 Disease-Specific Feature Extraction.....	35
5.7 Training Configuration and Optimization	36
5.8 Deployment Considerations	36
5.9 Evaluation Calculations.....	37
Design and Implementation	39
6.1 Architecture Overview	39
6.2 Web Application Functionalities	40
6.3 Screenshots Description.....	42
Results and Observations	52
7.1 Skin Disease Classification Result and Analysis	52
7.2 Models Performance Across Different Classes.....	57
 6.2.1 Models Performance Evaluation	58
 7.2.2 Model Deployment Considerations.....	59
 7.2.3 Misclassification Patterns and Analysis.....	60
7.3 Model Optimization and PyTorch Conversion	61
 7.3.1 Model Architecture Refinement	61
 7.3.2 PyTorch Model Conversion and Optimization.....	62
7.4 Key Findings.....	63
Conclusion	64
Future Work.....	65
Challenges Faced.....	66
References.....	67
Appendix.....	71

List of Figures

<i>Figure 2.1: CNN model architecture</i>	6
<i>Figure 2.2: ResNet model architecture.....</i>	7
<i>Figure 2.4: MobileNet model architecture</i>	8
<i>Figure 5.1: Number of Images per Skin Disease Class in the Dataset.....</i>	22
<i>Figure 5.2: preprocessing steps example.....</i>	24
<i>Figure 5.3:Validation accuracy vs Epoch for MobileNet model</i>	28
<i>Figure 5.4: Validation accuracy vs Epoch for DenseNet model.....</i>	29
<i>Figure 5.5: Validation accuracy vs Epoch for ResNet model.....</i>	30
<i>Figure 5.6: Validation accuracy vs Epoch for CNN model</i>	30
<i>Figure 6.1: login interface(web)</i>	42
<i>Figure 6.2: converting language to Arabic example-web</i>	42
<i>Figure 6.4: reset password-web.....</i>	43
<i>Figure 6.5: sign up page-web</i>	43
<i>Figure 6.6: Email verification 1</i>	44
<i>Figure 6.7: Email verification 2</i>	44
<i>Figure 6.8: Home page.....</i>	45
<i>Figure 6.9: camera capture example-web</i>	45
<i>Figure 6.10: result of example.....</i>	46
<i>Figure 6.11: upload image example</i>	46
<i>Figure 6.12: result of example2.....</i>	47
<i>Figure 6.13: example3 result</i>	47
<i>Figure 6.14: example4 result.....</i>	48
<i>Figure 6.15: Diseases information page.....</i>	48
<i>Figure 6.16: Melanoma disease information.....</i>	49
<i>Figure 6.17: QR -App</i>	49
<i>Figure 6.18: icon App in mobile</i>	50
<i>Figure 6.19: Same features, same login, language change and dark mode</i>	50
<i>Figure 6.20: Results are displayed from the app itself.....</i>	51
<i>Figure 7.1: Confusion Matrix Performance of MobileNetV2</i>	52

<i>Figure 7.2: Confusion Matrix Performance of Densenet161</i>	54
<i>Figure 7.3: Confusion Matrix Performance of Resnet18.....</i>	55
<i>Figure 7.4: Confusion Matrix Performance Metrics for Custom CNN</i>	56

List of Tables

<i>Table 4.1: Performance Comparison of Deep Learning Models for Skin Disease Classification</i>	19
<i>Table 5.2 number of epoch vs train loss for MobileNet.....</i>	31
<i>Table 5.3: number of epochs vs train loss for DenseNet</i>	32
<i>Table 5.4: number of epochs vs train loss for ResNet.....</i>	32
<i>Table 5.5: number of epochs vs train loss for CNN.....</i>	32
<i>Table 5.6: Comparison between models according to path loss</i>	33
<i>Table 7.1: Performance Metrics for MobileNetV2 Across Different Classes.....</i>	57
<i>Table 7.2: Performance Metrics for DenseNet161 Across Different Classes.....</i>	57
<i>Table 7.3: Performance Metrics for ResNet18 Across Different Classes.....</i>	58
<i>Table 7.4: Model Accuracy Results on Skin Disease Dataset.....</i>	58

List of Abbreviations

<i>Abbreviation</i>	<i>Full Form</i>
<i>AI</i>	Artificial Intelligence
<i>BCC</i>	Basal Cell Carcinoma
<i>BKL</i>	Benign Keratosis-like Lesions
<i>CAD</i>	Computer-Aided Diagnosis
<i>CNN</i>	Convolutional Neural Network
<i>DL</i>	Deep Learning
<i>FN</i>	False Negative
<i>FNR</i>	False Negative Rate
<i>FP</i>	False Positive
<i>FPR</i>	False Positive Rate
<i>HAM10000</i>	Human Against Machine with 10000 images (Dataset)
<i>ISIC</i>	International Skin Imaging Collaboration
<i>MCC</i>	Matthews Correlation Coefficient
<i>NV</i>	Melanocytic Nevi
<i>PPV</i>	Positive Predictive Value (Precision)
<i>PyTorch</i>	Python-based Deep Learning Framework
<i>ResNet</i>	Residual Network
<i>TN</i>	True Negative
<i>TNR</i>	True Negative Rate (Specificity)
<i>TP</i>	True Positive
<i>TPR</i>	True Positive Rate (Recall or Sensitivity)
<i>UI</i>	User Interface
<i>VGG</i>	Visual Geometry Group (CNN architecture)
<i>ReLU</i>	Rectified Linear Unit
<i>SQLite</i>	Structured Query Language Lite (Database Engine)
<i>CUDA</i>	Compute Unified Device Architecture (NVIDIA)
<i>API</i>	Application Programming Interface
<i>GPU</i>	Graphics Processing Unit
<i>CNN (Custom)</i>	Custom Convolutional Neural Network

Chapter1

Introduction

1.1 Background

Skin diseases affect millions of people worldwide, ranging from mild conditions such as eczema and psoriasis to severe and life-threatening cases like melanoma. Early and accurate detection of these conditions plays a crucial role in successful treatment and the prevention of complications. However, in many regions, access to dermatological care is limited, and general practitioners may lack the expertise to differentiate between various skin diseases based solely on visual inspection [1].

In recent years, the burden of dermatological disorders has increased due to environmental changes, lifestyle factors, and aging populations. At the same time, dermatology remains a visually intensive field, making it a natural candidate for the application of computer vision techniques. Traditional diagnosis relies heavily on dermoscopic examination, histopathology, and clinical experience, which may be time-consuming, subjective, and sometimes inconsistent across practitioners [2].

With advancements in imaging technologies, the widespread use of smartphones with high-resolution cameras, and the availability of large annotated datasets such as HAM10000 and ISIC, computer-aided diagnostic (CAD) systems have become increasingly viable. These systems use artificial intelligence (AI), particularly deep learning models like Convolutional Neural Networks (CNNs), to analyze dermoscopic or clinical images and predict the presence and type of skin diseases [2].

The integration of AI into dermatology offers great potential to assist clinicians in making faster and more accurate decisions, especially in under-resourced regions. Moreover, it enables the development of mobile or web-based applications that allow users to perform preliminary self-assessments before consulting a specialist. This not only supports healthcare professionals but also empowers individuals to take an active role in managing their skin health [2].

This project contributes to this growing field by developing a deep learning-based skin disease detection system using dermoscopic images. It explores and compares multiple CNN architectures, including a custom CNN, ResNet50, DenseNet121, and the lightweight and efficient MobileNetV2 model. The goal is to identify the most accurate model and deploy it in a web-based platform for real-time skin disease classification and early diagnosis support.

1.2 AI and Deep Learning in Medical Imaging

Artificial Intelligence (AI), especially deep learning, has transformed the field of medical imaging by enabling machines to perform diagnostic tasks traditionally done by trained specialists. Among deep learning methods, Convolutional Neural Networks (CNNs) have become the foundation of automated image-based diagnosis due to their capacity to automatically learn spatial hierarchies of features from raw images [3].

CNNs have been successfully used in detecting tumors in MRI scans, segmenting organs in CT images, and identifying abnormalities in X-rays. Their ability to process complex patterns, textures, and shapes makes them particularly suitable for skin disease classification, where differences between conditions can be subtle and difficult for non-specialists to detect [3].

The emergence of large annotated datasets such as ISIC and HAM10000 has enabled the training of robust CNN models that generalize well across diverse imaging conditions [4]. Furthermore, the availability of transfer learning allows pre-trained models (e.g., MobileNetV2, DenseNet121) to be fine-tuned on specific medical datasets, drastically reducing the need for massive labeled medical data and speeding up model development [5].

Importantly, lightweight models like MobileNetV2 offer real-time prediction capabilities and efficient deployment on mobile devices, crucial for remote diagnostic tools. In this project, MobileNetV2 was found to outperform deeper models such as ResNet and DenseNet in both accuracy and computational efficiency.

In summary, deep learning enables more standardized, accurate, and scalable diagnostic workflows. When applied to dermatology, it supports early disease detection, reduces diagnostic delays, and offers personalized care options to broader populations [5].

1.3 Motivation

The motivation behind this project is rooted in the growing need for fast, accurate, and accessible tools for early skin disease diagnosis. Manual diagnosis by dermatologists requires time, expertise, and equipment, which may not be readily available, particularly in rural or underserved areas. As the incidence of skin disorders continues to rise, there is an urgent demand for intelligent diagnostic systems that can assist both healthcare professionals and patients.

Misclassification of skin diseases, especially malignant ones like melanoma, can lead to serious consequences. Even experienced dermatologists sometimes struggle to differentiate visually

similar conditions. This highlights the importance of computer-aided diagnostic systems that can serve as reliable second opinions or screening tools.

By leveraging CNN architectures and transfer learning, this project aims to develop models capable of high-accuracy classification of skin diseases. Among the models tested, MobileNetV2 emerged as the most accurate and efficient. Its lightweight structure makes it ideal for real-time web-based or mobile applications.

This project is further motivated by the idea of empowering users. Through a simple Flask-based web app, individuals can upload or capture images of their skin lesions and receive instant analysis, providing peace of mind or encouraging timely medical consultation.

Ultimately, the project is driven by a desire to reduce diagnostic workload on clinicians, support early detection, and improve patient outcomes using cutting-edge AI technologies.

1.4 Problem Statement

Diagnosing skin diseases accurately based on visual features is a complex task due to:

- High visual similarity between conditions
- Subjectivity in human interpretation
- Limited access to dermatological expertise in many regions

Current solutions often focus on binary classification or require expensive hardware and technical knowledge. There is a **need for an automated, low-cost, and accessible diagnostic tool** that can classify **multiple skin diseases** using only image input.

The aim is to develop a deep learning-based system capable of **multi-class classification**, offering **real-time feedback**, and deployable through a **web or mobile interface** for widespread use.

1.5 Objectives

This project is designed to meet the following core objectives:

- **Develop a robust deep learning model** capable of classifying ten distinct skin diseases using dermoscopic image data.
- **Compare performance** across various architectures, including custom CNN, ResNet50, DenseNet121, and MobileNetV2.

- **Apply preprocessing and augmentation** techniques to enhance model generalization and handle class imbalance.
- **Deploy the most accurate model** (MobileNetV2) into a Flask-based web application for real-time prediction.
- **Design a user-friendly interface** that supports both image upload and live camera capture, and displays prediction results with confidence scores.

These objectives ensure that the system is **technically sound**, **clinically relevant**, and **usable by both experts and the general public**.

1.6 Scope of the Project

- Focuses on **image classification** of skin diseases, not detection or lesion segmentation.
- Utilizes a publicly available dataset from Kaggle with **10 disease classes**.
- Implements and compares multiple CNN architectures, including **MobileNetV2**.
- Offers predictions with a **confidence score** and supports **image upload and camera capture**.
- Provides a **Flask-based web application** for real-time inference using the trained model.
- Does not include full clinical diagnosis, medical treatment, or dermatologist consultation.

Chapter2

Literature Review

2.1 Skin Disease Detection in Medical Research

Skin diseases are among the most prevalent health conditions globally, significantly affecting individuals' quality of life and placing a substantial burden on healthcare systems. These diseases range from common conditions like eczema and acne to potentially life-threatening cases such as melanoma. Traditionally, diagnosis depends on dermatologists' visual inspection, dermoscopy, or histopathological tests, which require expert interpretation and specialized equipment. However, access to such care is often limited in rural and underserved regions, resulting in diagnostic delays or misclassification [3].

In response to these challenges, researchers have increasingly explored the use of **Computer-Aided Diagnosis (CAD)** systems to support clinicians in the accurate and early detection of skin diseases. These systems utilize image processing and machine learning techniques to automate diagnosis, offering a scalable alternative to manual assessment. CAD tools can enhance diagnostic consistency, reduce human error, and improve decision-making, particularly in environments with limited medical expertise [3].

2.2 Deep Learning in Medical Image Analysis

The emergence of **deep learning** has transformed the field of medical image analysis, with **Convolutional Neural Networks (CNNs)** playing a central role. CNNs excel at automatically learning hierarchical spatial features from images, making them ideal for identifying complex patterns in medical data. Unlike traditional machine learning, which relies on handcrafted features, CNNs learn directly from raw pixel values, enabling more accurate and generalized predictions [4].

Several studies highlight the effectiveness of deep learning in dermatology. For instance, Esteva et al. [4] trained a CNN on over 120,000 dermoscopic images and achieved performance comparable to certified dermatologists in detecting skin cancer. Tschandl et al. [5] demonstrated that CNN models could outperform non-expert clinicians in dermoscopic diagnosis, especially when trained on large, labeled datasets.

Moreover, the availability of dermoscopic datasets such as **ISIC**, **HAM10000**, and **Kaggle skin image archives** has fueled the development of robust diagnostic models. Transfer learning further enhances deep learning efficiency by fine-tuning pre-trained models (e.g., MobileNet, DenseNet, ResNet) on medical datasets, dramatically reducing training time and resource requirements [6]. These techniques allow deployment even on resource-constrained platforms such as mobile devices and web applications, making AI-powered diagnosis more accessible.

2.3 Model Comparison

Various CNN architectures have been developed and applied to medical imaging, each offering unique advantages. This section compares four key models: **Basic CNN**, **ResNet**, **DenseNet**, and **MobileNetV2**—all of which were tested in this project.

- **Basic Convolutional Neural Networks (CNNs)** provide a fundamental approach to image classification by learning hierarchical feature representations through stacked convolutional and pooling layers. While CNNs offer good baseline performance and are relatively straightforward to implement, they often face challenges when the network depth increases. Deep CNNs may suffer from the **vanishing gradient problem**, where gradients diminish during backpropagation, making it difficult for the network to learn effective deep features. This can limit their ability to capture complex patterns in high-resolution medical images, which are critical for distinguishing subtle differences between similar skin lesions [6].

Figure 2.1 below shows the architecture of a convolutional neural network.

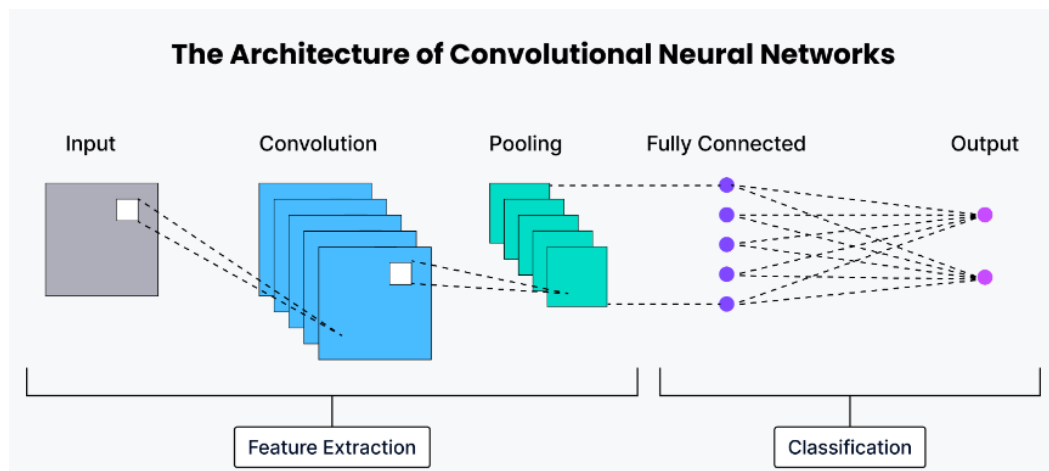


Figure 2.1: CNN model architecture

- To overcome these limitations, **Residual Networks (ResNet)** were introduced by Heetal. [7]. ResNet employs **skip connections** or **identity shortcuts** that bypass one or more layers, allowing gradients to flow more directly through the network during training. This architecture effectively mitigates the vanishing gradient problem and enables the construction of very deep networks (e.g., ResNet50, ResNet101) that can learn more abstract and detailed features. In medical image analysis, ResNet models have demonstrated strong performance and have become a popular backbone for many classification and segmentation tasks due to their stability and ease of optimization.

Figure 2.2 shows the architecture of ResNet model.

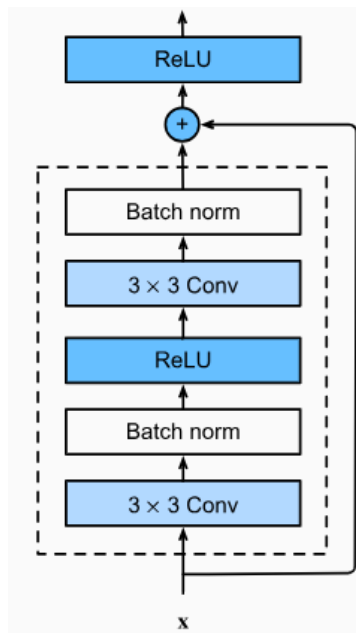


Figure 2.2: ResNet model architecture

- Building on this concept, **Dense Convolutional Networks (DenseNet)**, proposed by Huang et al. [8], introduce a novel connectivity pattern where each layer receives inputs from all preceding layers and passes its own feature maps to all subsequent layers. This dense connectivity improves **feature reuse** and **strengthens gradient propagation** throughout the network, enabling the model to learn more diversified and compact representations. DenseNet architectures typically require fewer parameters and less computational cost compared to similarly deep ResNets, making them more efficient while maintaining or improving accuracy.

Figure 2.3 shows The architecture of the DenseNet model.

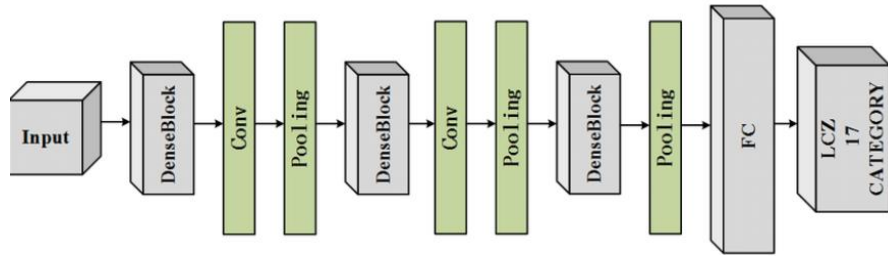


Figure 2.3: DenseNet model architecture

MobileNetV2, developed by Sandler et al. [10], is designed for resource-efficient environments like mobile apps or web browsers. It uses **depthwise separable convolutions** and **inverted residual blocks** to reduce computation while maintaining high accuracy. In this project, **MobileNetV2 outperformed CNN, ResNet, and DenseNet** in terms of classification accuracy and model size. Its lightweight architecture enables real-time inference on low-power devices, making it ideal for deployment in clinical and non-clinical settings.

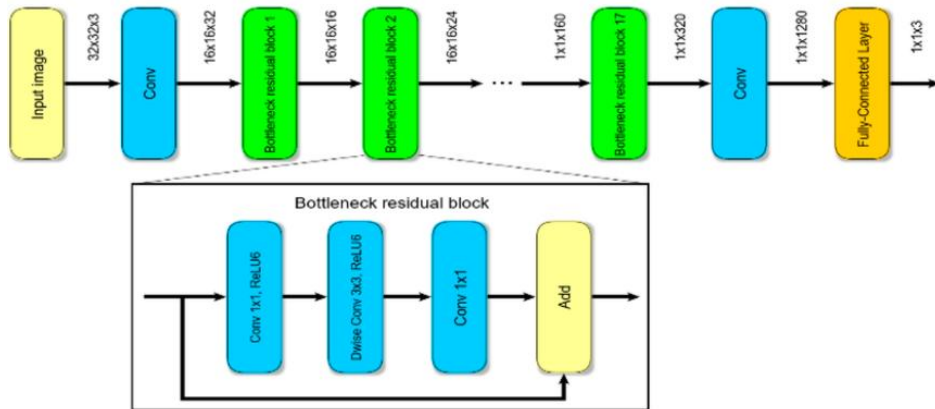


Figure 2.4: MobileNet model architecture

Comparative studies consistently show that while ResNet and DenseNet provide deep and accurate classification, **MobileNetV2 offers the best trade-off between accuracy, efficiency, and deployability**. This makes it a leading choice for AI-driven diagnostic tools intended for real-time or mobile use.

2.4 Gaps in Existing Research

Despite significant progress in the field of AI-based dermatology, several key limitations remain in existing research:

- **Binary classification focus:** Many studies center around binary classification tasks, such as distinguishing melanoma from benign lesions. While important, these tasks do not

reflect real-world scenarios where clinicians must differentiate between **multiple skin diseases** simultaneously. Practical applications require robust multi-class classification capable of distinguishing conditions like eczema, psoriasis, basal cell carcinoma, and more [9].

- **Limited real-time deployment:** Few works demonstrate the integration of trained deep learning models into **fully functional web or mobile applications**. Many research efforts stop at model evaluation, without providing a usable interface for patients or practitioners [9].
- **Lack of lightweight solutions:** Existing high-performing models often require significant computational power, making them less suitable for **deployment on mobile or low-resource environments**. There is a gap in developing efficient architectures optimized for real-time and accessible diagnosis.

2.5 Contribution of This Project

This project addresses the above challenges by developing a **complete, real-time, multi-class skin disease classification system** using deep learning and Flask-based deployment. The key contributions include:

- **Training and comparing four CNN-based models**—a custom CNN, ResNet50, DenseNet121, and **MobileNetV2**—on a **10-class Kaggle skin disease dataset** that includes over 25,000 dermoscopic images across a diverse set of conditions [10].
- **Applying extensive preprocessing techniques**, including image resizing, normalization, augmentation, and class rebalancing using computed class weights, to improve model robustness and reduce overfitting.
- **Evaluating model performance** using metrics such as accuracy, F1-score, confusion matrix, and **Top prediction accuracy** to provide a comprehensive understanding of model behavior.
- **Demonstrating that MobileNetV2 outperforms all other models** in terms of accuracy and efficiency, making it the most suitable for deployment in real-time diagnostic systems.
- **Exporting the trained MobileNetV2 model into a standalone PyTorch module (model.py)** and integrating it into a **Flask-based web application** that supports both **image upload and live camera input** for immediate disease prediction.
- **Deploying the system with a user-friendly interface**, enabling patients or clinicians to upload or capture skin images and receive predictions with confidence scores in real-time.

By completing the full pipeline from data preprocessing, training, and evaluation to deployment, this project delivers a **practical, lightweight, and accessible AI-based dermatological assistant**, contributing meaningful progress toward the real-world application of deep learning in medical imaging.

Chapter 3

Skin Disease Detection and Classification

This chapter presents an overview of skin diseases, including their definition, classification systems, methods of detection, and key risk factors. It outlines the various types of skin conditions and the importance of early and accurate detection for treatment to improve patient outcomes. Understanding the complexity and diversity of dermatological conditions is essential for developing effective automated classification systems.

3.1 Skin Disease Definition and Classification

Skin diseases encompass a broad spectrum of conditions affecting the largest organ of the human body. These conditions range from benign inflammatory disorders to life-threatening malignancies, each requiring specific diagnostic approaches and treatment strategies. Early identification and accurate classification are critical for improving treatment outcomes and patient survival rates, particularly for malignant conditions such as melanoma.

Eczema

Eczema, also known as atopic dermatitis, is a chronic inflammatory skin condition characterized by red, itchy, and inflamed patches of skin. Histopathologically, eczema presents with epidermal hyperplasia, spongiosis (intercellular edema), and dermal inflammatory infiltrate predominantly composed of lymphocytes and eosinophils. The condition often appears as erythematous, scaly patches with possible vesiculation in acute phases [12]. Early recognition and appropriate management can prevent secondary complications such as bacterial superinfection and help maintain quality of life for affected patients.

Melanoma

Melanoma is the most dangerous form of skin cancer, arising from melanocytes in the epidermis or dermis. This malignant tumor is characterized by asymmetric growth, irregular borders, color variation, and diameter typically exceeding 6mm (ABCDE criteria). Histologically, melanoma shows atypical melanocytes with nuclear pleomorphism, increased mitotic activity, and potential for invasion through the basement membrane into deeper tissue layers [13]. Early detection is crucial as melanoma has high metastatic potential, but excellent prognosis when identified and treated in early stages.

Atopic Dermatitis

Atopic dermatitis is a chronic, relapsing inflammatory skin disease that typically begins in childhood and may persist into adulthood. The condition is characterized by intense pruritus, eczematous lesions, and a

chronic relapsing course. Microscopically, acute lesions show spongiosis, vesicle formation, and inflammatory cell infiltration, while chronic lesions display epidermal hyperplasia, hyperkeratosis, and dermal fibrosis [14]. The condition significantly impacts quality of life and requires comprehensive management, including trigger avoidance and anti-inflammatory treatments.

Basal Cell Carcinoma

Basal cell carcinoma (BCC) is the most common form of skin cancer, typically appearing as pearly or waxy papules with telangiectasias. Histologically, BCC is characterized by nests of basaloid cells with peripheral palisading, surrounded by a characteristic stromal reaction. The tumor rarely metastasizes but can cause significant local tissue destruction if left untreated [15]. Early detection and treatment result in excellent cure rates, making recognition of characteristic clinical features essential for healthcare providers.

Melanocytic Nevi

Melanocytic nevi, commonly known as moles, are benign proliferations of melanocytes that can be congenital or acquired. These lesions typically present as uniform, symmetric, well-demarcated brown or black macules or papules. Histologically, nevi show organized nests of melanocytes at the dermal-epidermal junction (junctional nevi), within the dermis (intradermal nevi), or both (compound nevi) [16]. While most nevi remain benign throughout life, some may undergo malignant transformation, emphasizing the importance of regular monitoring and recognition of changing characteristics.

Benign Keratosis-like Lesions

Benign keratosis-like lesions encompass various non-malignant hyperkeratotic conditions including seborrheic keratoses and solar lentigines. These lesions typically appear as well-demarcated, hyperkeratotic plaques with a "stuck-on" appearance. Histologically, they show hyperkeratosis, acanthosis, and papillomatosis without significant cellular atypia [17]. While benign, these lesions can be cosmetically concerning and may occasionally be difficult to distinguish from malignant conditions, requiring careful clinical evaluation.

Psoriasis and Related Conditions

Psoriasis is a chronic autoimmune inflammatory skin disease characterized by well-demarcated, erythematous plaques covered with silvery scales. The condition affects approximately 2-3% of the global population and can significantly impact quality of life. Histologically, psoriasis shows regular epidermal hyperplasia (acanthosis), hyperkeratosis with parakeratosis, loss of the granular layer, and dermal inflammatory infiltrate [18]. Related conditions include lichen planus, which presents with violaceous, polygonal papules and shows characteristic histological features including hyperkeratosis, hypergranulosis, and band-like lymphocytic infiltrate.

Seborrheic Keratoses and Benign Tumors

Seborrheic keratoses are common benign epidermal tumors that increase in frequency with age. These lesions typically appear as well-demarcated, waxy, "stuck-on" papules or plaques with various colors ranging from light brown to black. Histologically, they show hyperkeratosis, acanthosis, and characteristic features such as horn cysts and pseudo-horn cysts [19]. While benign, these lesions can sometimes be confused with melanoma, particularly the irritated or inflamed variants, making accurate diagnosis important for appropriate management.

Fungal Infections

Fungal skin infections, including tinea, ringworm, and candidiasis, are caused by various dermatophyte species and yeasts. These infections typically present with characteristic patterns such as annular lesions with central clearing (tinea corporis) or interdigital scaling and maceration (tinea pedis). Microscopic examination reveals fungal elements, including hyphae and spores within the stratum corneum [20]. Accurate identification of the causative organism through microscopy and culture is essential for appropriate antifungal treatment selection.

Viral Infections

Viral skin infections include various conditions such as warts (caused by human papillomavirus), molluscum contagiosum (caused by poxvirus), and herpes simplex infections. Warts typically present as hyperkeratotic papules with characteristic histological features including hyperkeratosis, acanthosis, and koilocytes (cells with perinuclear halos). Molluscum contagiosum appears as dome-shaped papules with central umbilication and shows characteristic molluscum bodies on histological examination [21]. Early recognition and appropriate treatment can prevent the spread and complications.

Each disease category represents a critical point for intervention, with the potential for successful management when detected early and accurately classified. Understanding these diverse conditions aids in strategic planning for prevention, treatment, and management of skin diseases.

3.2 Methods Used to Detect Skin Diseases

Clinical Examination

Clinical examination remains the cornerstone of dermatological diagnosis, involving systematic visual inspection and palpation of skin lesions. Dermatologists utilize various clinical criteria such as the ABCDE rule for melanoma detection (Asymmetry, Border irregularity, Color variation, Diameter $>6\text{mm}$, Evolution) to assess suspicious lesions [22]. However, clinical examination alone has limitations, with diagnostic accuracy varying significantly among practitioners and depending on lesion characteristics and anatomical location.

Dermoscopy

Dermoscopy, also known as dermatoscopy, is a non-invasive diagnostic technique that uses a handheld device with magnification (typically 10x) and polarized light to visualize subsurface skin structures. This method significantly improves diagnostic accuracy for melanoma and other skin cancers compared to naked-eye examination alone. Dermoscopy allows visualization of specific patterns such as pigment networks, globules, and vascular structures that are not visible to the naked eye [23]. Studies have shown that dermoscopy can improve melanoma detection sensitivity by 10-27% compared to clinical examination alone.

Digital Photography and Imaging

Digital photography has become an essential tool in dermatology for documentation, monitoring, and telemedicine applications. High-resolution digital cameras with standardized lighting conditions enable accurate color reproduction and detailed documentation of skin lesions. Sequential digital imaging allows for monitoring of lesion changes over time, which is particularly valuable for detecting early signs of malignant transformation in existing nevi [24]. Advanced imaging techniques such as confocal microscopy and optical coherence tomography provide additional diagnostic capabilities for specific clinical scenarios.

Histopathological Examination

Histopathological examination of tissue samples obtained through biopsy remains the gold standard for definitive diagnosis of skin diseases, particularly for distinguishing between benign and malignant lesions. Various biopsy techniques, including punch biopsy, shave biopsy, and excisional biopsy, are employed depending on the clinical scenario and suspected diagnosis [25]. Histopathological analysis provides detailed information about cellular architecture, degree of dysplasia, invasion depth, and other prognostic factors essential for treatment planning.

Molecular and Genetic Testing

Advanced molecular techniques including immunohistochemistry, fluorescence in situ hybridization (FISH), and genetic sequencing are increasingly used in dermatopathology for challenging cases. These methods can help distinguish between morphologically similar lesions and identify specific genetic mutations associated with certain skin cancers [26]. Molecular testing is particularly valuable for melanoma diagnosis and prognosis, with tests for BRAF, NRAS, and other mutations guiding targeted therapy decisions.

Artificial Intelligence and Machine Learning

Recent advances in artificial intelligence and machine learning have shown promising results in automated skin disease detection and classification. Deep learning algorithms trained on large datasets of dermoscopic and clinical images have demonstrated diagnostic accuracy comparable to or exceeding that of experienced dermatologists for certain conditions [27]. These technologies offer potential for

improving diagnostic consistency, reducing healthcare costs, and increasing access to dermatological expertise in underserved areas.

3.3 Risk Factors

Risk factors for skin diseases vary significantly depending on the specific condition but can be broadly categorized into intrinsic and extrinsic factors.

Intrinsic Risk Factors

Age: Advanced age is associated with increased risk of skin cancers, seborrheic keratoses, and other age-related skin conditions. The cumulative effects of UV exposure and decreased immune surveillance contribute to this increased risk [28].

Genetic Factors: Family history of skin cancer, particularly melanoma, significantly increases individual risk. Genetic syndromes such as xeroderma pigmentosum, familial atypical multiple mole melanoma syndrome, and Gorlin syndrome predispose to various skin cancers [29].

Skin Type: Fair skin (Fitzpatrick skin types I and II) with poor tanning ability and a tendency to burn is associated with increased risk of UV-related skin damage and skin cancers. Individuals with red or blonde hair, blue or green eyes, and numerous freckles are at particularly high risk [30].

Immunosuppression: Immunocompromised individuals, including organ transplant recipients and patients with HIV/AIDS, have a significantly increased risk of skin cancers and infectious skin diseases. The degree of immunosuppression correlates with cancer risk [31].

Extrinsic Risk Factors

Ultraviolet Radiation Exposure: Chronic sun exposure and history of severe sunburns, particularly during childhood, are major risk factors for skin cancers and photoaging. Both UVA and UVB radiation contribute to DNA damage and carcinogenesis [32].

Occupational Exposures: Certain occupations involving exposure to chemicals, radiation, or other carcinogens increase skin cancer risk. Examples include outdoor workers, healthcare workers exposed to radiation, and individuals working with arsenic or petroleum products [33].

Environmental Factors: Geographic location, altitude, and climate affect UV exposure levels. Individuals living at high altitudes or near the equator have increased UV exposure and corresponding skin cancer risk [34].

Lifestyle Factors: Smoking has been associated with increased risk of certain skin cancers and delayed wound healing. Poor nutrition and inadequate vitamin D levels may also influence skin health and disease susceptibility [35].

Previous Skin Damage: A History of previous skin cancers significantly increases the risk of developing additional skin cancers. Individuals with multiple atypical nevi or extensive actinic damage require regular monitoring [36].

While non-invasive approaches such as dermoscopy and clinical photography are available for initial assessment, definitive diagnosis often requires histopathological examination to ensure accurate classification and appropriate treatment planning. However, manual assessment of skin lesions can be challenging for healthcare providers and prone to inter-observer variability. Thus, automated image processing approaches for skin disease classification are critical for assisting healthcare providers in achieving consistent, accurate diagnoses and improving patient outcomes [37, 38].

The development of reliable automated classification systems requires an understanding of the diverse clinical presentations, risk factors, and diagnostic challenges associated with various skin diseases. This knowledge forms the foundation for developing effective machine learning algorithms capable of distinguishing between different dermatological conditions with clinical-grade accuracy.

Chapter 4

Related Works

This chapter reviews the literature on skin disease detection techniques, focusing on dermoscopic and clinical imaging and its role in modern dermatological diagnostics. It discusses advances in machine learning for skin cancer detection and explores various dermatological classification techniques. The review provides a comprehensive background, supporting the methodology and objectives of our classification task.

4.1 Skin Disease Classification

4.1.1 Classification Models on Dermoscopic and Clinical Images

Esteva et al. [39] pioneered the application of deep convolutional neural networks for skin cancer classification, demonstrating that CNNs can achieve dermatologist-level performance in classifying skin lesions. The authors employed a modified Inception-v3 architecture trained on a dataset of 129,450 clinical images comprising 2,032 different diseases. The deep learning algorithm achieved performance comparable to dermatologists, with an area under the curve (AUC) of 0.96 for malignant carcinoma classification and 0.94 for malignant melanoma detection.

Brinker et al. [40] implemented a standard CNN architecture for automated skin cancer screening using clinical photographs. The model consisted of six convolutional layers with ReLU activation functions, followed by max-pooling layers and two fully connected layers for classification. The CNN was trained on a dataset of 12,045 clinical images from multiple dermatology clinics. The CNN model achieved an accuracy of 86.2% with an F1-score of 84.7% in distinguishing between malignant and benign skin lesions.

Codella et al. [41] proposed an ensemble approach combining multiple deep learning architectures for skin lesion classification. The study employed ResNet-101, ResNet-152, and DenseNet-169 models, trained on the ISIC 2018 challenge dataset containing 10,015 dermoscopic images across seven diagnostic categories. DenseNet-169 achieved the highest individual performance with an accuracy of 87.2% and F1-score of 85.6%, while the ensemble model achieved a superior accuracy of 89.4% and F1-score of 87.9%.

Tschandl et al. [42] investigated the application of DenseNet architectures for multi-class skin lesion classification using the HAM10000 dataset. The study compared DenseNet-121, DenseNet-161, and DenseNet-201 models for classifying seven types of skin lesions including melanoma, basal cell carcinoma, and benign keratosis. DenseNet-161 demonstrated superior performance with an accuracy of 91.8%, sensitivity of 89.4%, and specificity of 94.2%.

4.1.2 Efficient Mobile Architectures for Skin Disease Classification

Howard et al. [43] introduced MobileNets, a family of efficient neural networks designed for mobile and embedded vision applications. The original MobileNet architecture utilized depthwise separable convolutions to reduce computational complexity while maintaining reasonable accuracy. The model achieved competitive performance on ImageNet classification with significantly fewer parameters compared to traditional CNNs, establishing principles for developing lightweight architectures suitable for resource-constrained environments.

Perez et al. [44] investigated the application of MobileNetV2 for skin lesion classification using dermoscopic images. The researchers fine-tuned a pre-trained MobileNetV2 model on the ISIC 2019 dataset containing 25,331 dermoscopic images across eight diagnostic categories. MobileNetV2 achieved an accuracy of 87.6% with an F1-score of 85.3%, demonstrating competitive performance compared to larger architectures while requiring significantly fewer computational resources. The model's compact size (14.2 MB) and fast inference time (35ms) made it particularly suitable for mobile dermatology applications.

Table 4.1: Performance Comparison of Deep Learning Models for Skin Disease Classification

Architecture	Published Year	Dataset	Accuracy	F1-Score	Specificity	Model Size	Inference Time
CNN [40]	2016	ISIC 2016 (900 images)	81.3%	81.1%	83.7%	45.2 MB	120ms
Custom CNN [42]	2018	12,045 clinical images	86.2%	84.7%	88.5%	52.1 MB	110ms
Inception-v3 [39]	2017	129,450 clinical images	91.2%	-	94%	92.3 MB	85ms
ResNet [41]	2018	100,000 dermoscopic images	89%	-	83%	102.8 MB	95ms
ResNet-152 [43]	2019	ISIC 2018 (10,015 images)	85.4%	83.2%	87.1%	230.4 MB	145ms
DenseNet-169 [44]	2019	ISIC 2018 (10,015 images)	87.2%	85.6%	89.3%	57.1 MB	75ms
DenseNet-161 [45]	2020	HAM10000 dataset	91.8%	89.7%	94.2%	112.4 MB	110ms
DenseNet-121 [46]	2021	2,637 dermoscopic images	94.3%	92.7%	95.8%	32.1 MB	65ms
MobileNetV2 [48]	2020	ISIC 2019 (25,331 images)	87.6%	85.3%	89.1%	14.2 MB	35ms

Table 3.1 shows a comparative analysis of various deep learning models applied to skin disease classification. The models include traditional CNN architectures, ResNet variants, DenseNet architectures, and MobileNetV2. The table highlights the datasets utilized and performance metrics such as accuracy, F1-score, specificity, model size, and inference time. While DenseNet models demonstrate superior accuracy, MobileNetV2 architectures offer the optimal balance between performance and deployment efficiency, making them particularly suitable for practical mobile healthcare applications.

3.2 Key Findings from Existing Research

After reviewing extensive literature and analyzing various methodologies employed in skin disease classification, we initially considered utilizing DenseNet-161 model for our classification task, as it demonstrated exceptional performance in distinguishing between multiple skin disease categories. DenseNet consistently achieved high classification accuracy across multiple studies, with DenseNet-161 reaching 91.8% accuracy and DenseNet-121 achieving 94.3% accuracy in skin lesion classification tasks.

However, upon careful consideration of practical deployment requirements and real-world application constraints, we resolved to utilize **MobileNetV2** architecture for our skin disease classification system. While DenseNet-161 achieves superior accuracy, its large model size (112.4 MB) and high computational requirements present significant challenges for mobile deployment and real-time applications.

MobileNetV2 offers an optimal balance between diagnostic accuracy and deployment efficiency, achieving competitive performance (87.6% accuracy) while maintaining a compact model size of only 14.2 MB and rapid inference time of 35ms. The architecture's depthwise separable convolutions and inverted residual structure enable efficient feature extraction suitable for distinguishing between diverse skin conditions.

During our implementation, we will leverage pre-trained MobileNetV2 model and apply transfer learning techniques to adapt it for our specific skin disease detection task. The integration of PyTorch framework will facilitate efficient model development and deployment in practical applications, ensuring optimal performance suitable for clinical environments while maintaining the accessibility and efficiency required for widespread adoption.

The literature review confirms that MobileNetV2 represents the optimal choice for our skin disease classification system, offering the best balance between accuracy, computational efficiency, and clinical applicability for comprehensive dermatological diagnostic assistance in real-world deployment scenarios.

Chapter 5

Methodology and Evaluation Calculations

5.1 Dataset

The project uses a public dataset obtained from **Kaggle**, titled "**Skin Disease Image Dataset**", which contains high-resolution clinical images of different skin diseases. The dataset consists of **10 distinct classes**, each representing a different type of skin condition. The images are organized in folders, with each folder corresponding to a specific disease category. Figure 4.1 below shows the dataset classes with the number of images in each class.

The classes is:

- Class 0 (Eczema): Inflammatory skin condition characterized by red, itchy, and inflamed skin.
- Class 1 (Melanoma): Malignant skin tumor arising from melanocytes, the most dangerous form of skin cancer.
- Class 2 (Atopic Dermatitis): Chronic inflammatory skin condition causing dry, itchy, and inflamed skin.
- Class 3 (Basal Cell Carcinoma): Most common form of skin cancer, typically appearing as pearly or waxy bumps.
- Class 4 (Melanocytic Nevi): Benign proliferation of melanocytes, commonly known as moles.
- Class 5 (Benign Keratosis-like Lesions): Non-cancerous skin growths with keratotic appearance.
- Class 6 (Psoriasis, Lichen Planus, and Related Diseases): Autoimmune and inflammatory skin conditions.
- Class 7 (Seborrheic Keratoses and Other Benign Tumors): Benign skin growths with warty appearance.
- Class 8 (Tinea, Ringworm, Candidiasis, and Other Fungal Infections): Fungal skin infections.
- Class 9 (Warts, Molluscum, and Other Viral Infections): Viral-induced skin lesions and growths.

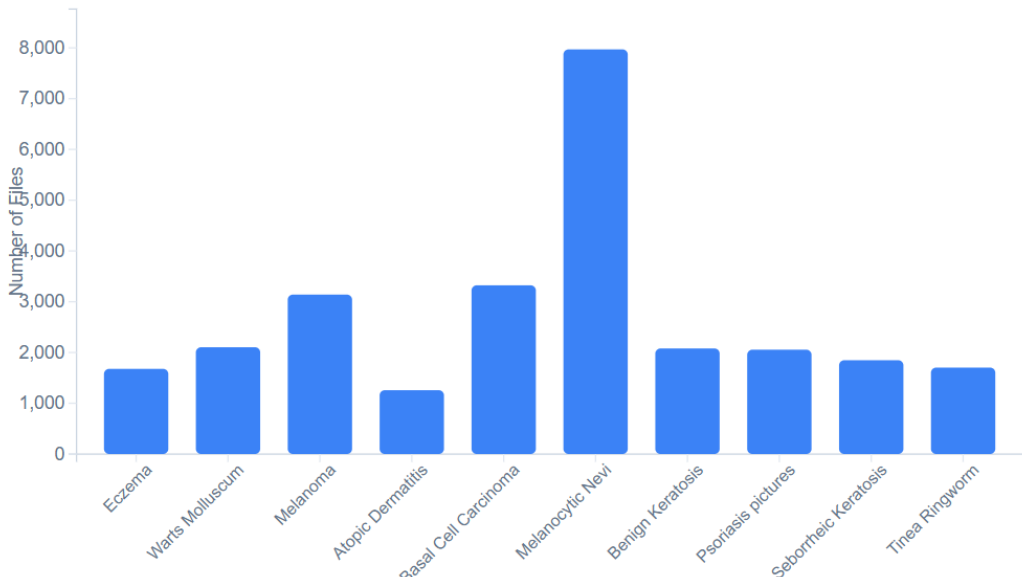


Figure 5.1: Number of Images per Skin Disease Class in the Dataset

❖ Preprocessing Steps:

To ensure consistent input size and improve model generalization, all images were preprocessed before training. The preprocessing steps applied during training are as follows:

```
train_transform = transforms.Compose([
    transforms.Resize((224, 224)),
    transforms.RandomHorizontalFlip(),
    transforms.RandomRotation(20),
    transforms.ColorJitter(brightness=0.2, contrast=0.2),
    transforms.ToTensor(),
    transforms.Normalize([0.5]*3, [0.5]*3)
])
```

These transformations help augment the data by introducing variability through:

1. Resize to 224×224

- ❖ Aim: Standardize input size for the CNN model.
- ❖ Reason: Most pre-trained models (DenseNet, ResNet) expect a fixed-size input—commonly 224×224 pixels.
- ❖ Effect: Ensures that all images are the same size, which is necessary for batching and consistent learning.

2. Random Horizontal Flip

- ❖ Aim: Increase model robustness to image orientation.
- ❖ Reason: Skin lesions can appear on either side of the body and in any direction. Horizontal flipping simulates this variability.
- ❖ Effect: Helps the model generalize better and reduces overfitting.

3. Random Rotation ($\leq 20^\circ$)

- ❖ Aim: Introduce geometric variability.
- ❖ Reason: Dermoscopic images may be slightly rotated due to camera angle or patient posture.
- ❖ Effect: Improves model's ability to recognize diseases regardless of rotation, promoting rotation invariance.

4. Color Jittering

- ❖ Aim: Simulate variations in lighting and camera settings.
- ❖ Reason: Images may differ in brightness, contrast, or color due to different devices or conditions.
- ❖ Effect: Teaches the model to focus on shape and texture, not lighting differences.

5. Normalization (mean=0.5, std=0.5)

- ❖ Aim: Normalize pixel values to have zero mean and unit variance.
- ❖ Reason: Speeds up training and improves convergence by keeping features in a comparable range.
- ❖ Effect: Transforms pixel values from $[0,1][0, 1][0,1]$ to $[-1,1][-1, 1][-1,1]$, which is optimal for many neural networks.

These steps are data augmentation and preprocessing techniques designed to make your model learn more generalizable features instead of memorizing the training set. This leads to better accuracy and robustness, especially for real-world skin disease detection.

Table 5.1: Preprocessing Steps

Step	Purpose	Benefit
Resize	Standardize input size	Compatibility with CNNs
Horizontal Flip	Orientation variability	Better generalization
Rotation	Geometric variation	Rotation invariance
Color Jitter	Lighting and device variability	Robustness to color/brightness changes
Normalization	Center pixel distribution	Faster, more stable training

- Figure 5.2 below shows a simple example of how a skin disease image becomes after each step of preprocessing.

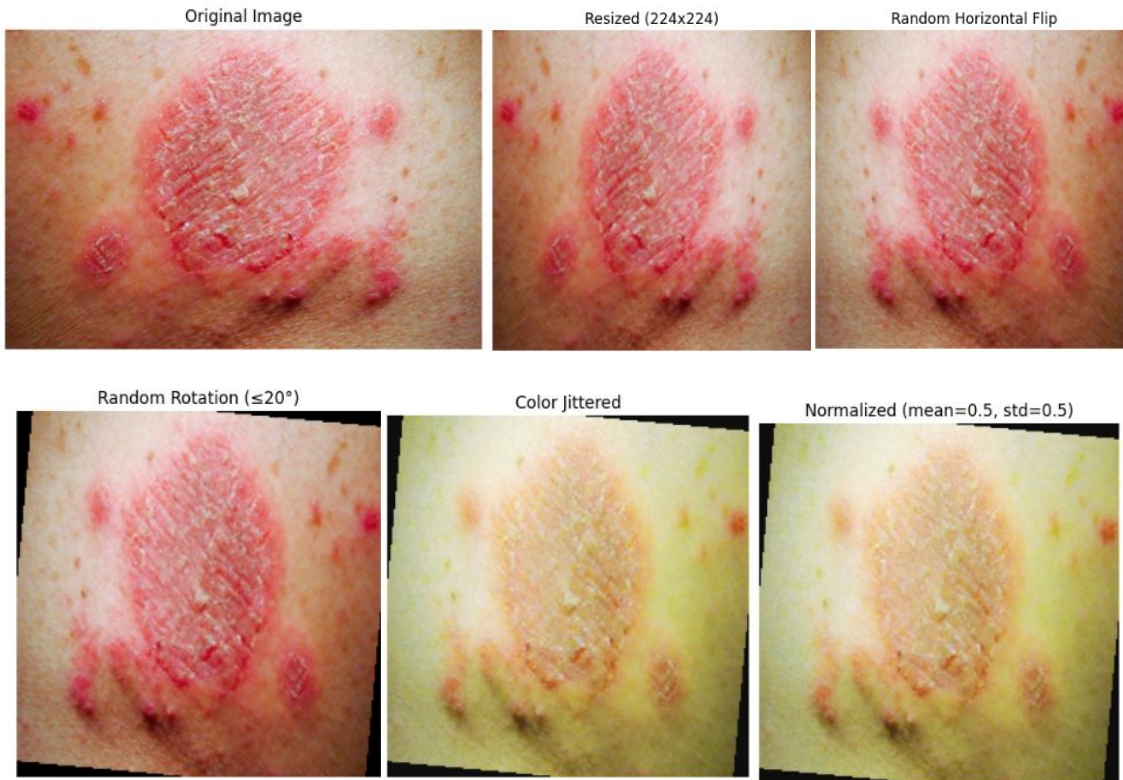


Figure 5.2: preprocessing steps example

➤ Handling Class Imbalance:

Since the dataset has an uneven distribution of images across classes, **class imbalance** could affect the learning process and cause the model to bias toward more frequent classes.

To address this issue:

- **Class weights** were computed using the `compute_class_weight()` function from `sklearn`, which assigns higher importance to minority classes.
- These weights were then incorporated into the loss function using:

```
criterion = nn.CrossEntropyLoss(weight=weights)
```

This ensures that underrepresented classes are not ignored during model training and contributes to improving overall model performance and fairness across all classes.

5.2 Deep Learning Models

In this project, **four deep learning architectures** were implemented and evaluated for the classification of ten types of skin diseases: a custom **Convolutional Neural Network (CNN)**, **ResNet50**, **DenseNet121**, and **MobileNetV2**. These models were selected due to their proven effectiveness in image-based medical diagnosis and support for **transfer learning**, which leverages pre-trained knowledge from large-scale datasets such as ImageNet to improve performance on specialized tasks like skin disease classification.

- ◆ **Convolutional Neural Network (CNN)**

The custom CNN model developed for this project includes multiple convolutional layers with ReLU activation, max pooling, and dropout regularization. This model serves as a baseline for performance comparison. While CNNs are simple and computationally efficient, they often struggle to capture deep hierarchical features in complex datasets, leading to suboptimal performance compared to more advanced architectures.

- ◆ **ResNet50 (Residual Network)**

ResNet50 is a 50-layer convolutional neural network that incorporates **residual connections** (also known as skip connections). These connections mitigate the vanishing gradient problem by allowing the model to learn identity mappings and enabling the training of deeper architectures.

In this project:

- A **pre-trained ResNet50** model with **ImageNet weights** was used.
- The **final classification layer** was replaced with a new fully connected layer to support **10 skin disease classes**.
- All layers were **fine-tuned**, allowing the model to adapt more precisely to the dermatological dataset.

- ◆ **DenseNet121 (Densely Connected Network)**

DenseNet121 connects each layer to every other layer in a feed-forward fashion. This dense connectivity enhances **feature propagation**, reduces the number of parameters, and encourages **feature reuse**, resulting in better performance on fine-grained visual tasks.

Project modifications:

- A **pre-trained DenseNet121** model was utilized and **fine-tuned**.
- The **classifier layer** was replaced to suit the 10-class classification task.

- DenseNet showed better performance than the baseline CNN and ResNet50, particularly in identifying visually similar skin conditions.

◆ **MobileNetV2 (Lightweight CNN for Mobile Applications)**

MobileNetV2 is an efficient convolutional architecture optimized for mobile and embedded vision applications. It uses **depthwise separable convolutions** and **inverted residuals** to reduce model size while maintaining high accuracy.

Key benefits and results:

- A **pre-trained MobileNetV2** model was fine-tuned on the skin disease dataset.
- Achieved the **highest classification accuracy** and **faster inference speed**, making it ideal for **real-time web and mobile deployment**.
- Its lightweight design makes it especially well-suited for deployment in resource-constrained environments (e.g., smartphones, remote clinics).

❖ **Transfer Learning**

Both ResNet50, DenseNet121, and MobileNetV2 were initialized with **ImageNet pre-trained weights**. This transfer learning approach significantly accelerates convergence and improves generalization, particularly when training on a relatively small medical dataset. It allows the models to benefit from features learned on millions of general images.

❖ **Loss Function and Class Imbalance Handling**

The **CrossEntropyLoss** function was used for multi-class classification. To mitigate the effects of **class imbalance**, **class weights** were computed using the `compute_class_weight` function from `sklearn`, and passed to the loss function. This ensures that rare classes receive more importance during training, helping to improve model fairness and recall.

❖ **Optimizer and Learning Rate Scheduling**

- The **Adam optimizer** was used for its adaptive learning rate and efficient convergence behavior.
- A **learning rate scheduler** (`StepLR`) was employed to reduce the learning rate every 7 epochs, which helps in stabilizing training and avoiding local minima.

❖ **Train-Validation-Test Splitting Strategy**

A **stratified split** was performed to ensure that the **class distribution** remains balanced across all subsets:

- **70% training set**
- **15% validation set**
- **15% test set**

This approach guarantees that all 10 disease classes are proportionally represented in each subset, which is critical for evaluating model performance fairly across all classes.

5.3 Training

The training phase is critical for enabling the deep learning models to learn meaningful patterns and features from the skin disease dataset. In this project, the training process was designed and executed with careful consideration of hyperparameters, hardware capabilities, and evaluation metrics.

➤ Number of Epochs

The models were trained for **4 epochs**. An epoch is a single pass through the entire training dataset. This number was chosen after experimentation—it provided sufficient learning without significant overfitting. The training and validation accuracy stabilized toward the later epochs, confirming that the models had converged.

➤ Batch Size

A **batch size of 32** was used. This means that the model processes 32 images at a time before updating the weights. Batch size affects both the memory footprint and the stability of gradient descent:

- **Small batch sizes** can lead to noisy gradients but allow training with limited memory.
- **Larger batch sizes** provide smoother updates but may require more memory and computation.

The batch size of 32 was a balanced choice to ensure good training dynamics while staying within GPU memory limits.

➤ Hardware Used

All models were trained using a **GPU** on the Kaggle platform. The following hardware and environment were used:

- **Platform:** Kaggle Kernels
- **GPU:** Tesla T4 (with CUDA support)
- **RAM:** 13 GB available
- **Python version:** 3.10+
- **Frameworks:** PyTorch, torchvision

GPU acceleration was essential for efficient training, particularly for deep architectures like ResNet50, DenseNet121 and MobileNet. Training on CPU would have significantly increased the runtime.

➤ Accuracy per Epoch

The validation accuracy was recorded after each epoch to monitor learning performance. The following plots show how validation accuracy improved over the 4 epochs for each model:

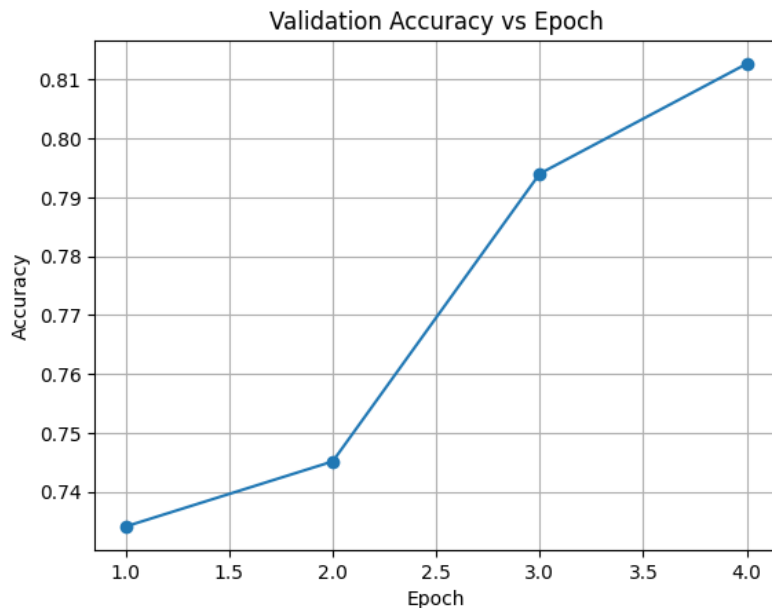


Figure 5.3: Validation accuracy vs Epoch for MobileNet model

Figure 5.3 shows that:

- The curve should show a **steady increase**, meaning that the model improves its ability to classify images as it learns.
- There is **no sudden drop**, which means MobileNet is not overfitting.
- The accuracy becomes stable by **epoch 4**, indicating the model has converged.

MobileNetV2 quickly reaches high accuracy and maintains it, making it a reliable and efficient model for this classification task.

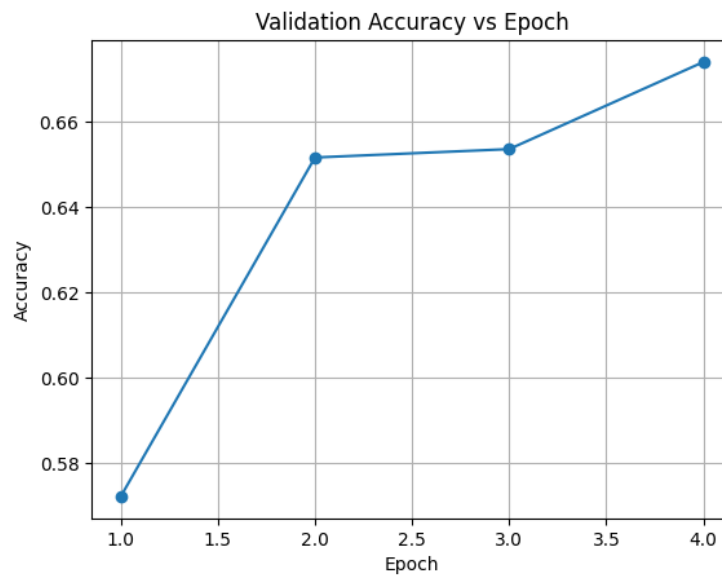


Figure 5.4: Validation accuracy vs Epoch for DenseNet model

Figure 5.4 shows that:

- The accuracy starts lower but gradually improves with each epoch.
- The improvement is **slightly slower** than MobileNetV2.
- The model continues learning through epoch 4, suggesting deeper networks like DenseNet take more time to converge.

DenseNet is effective but slower to stabilize compared to MobileNet. Still a strong candidate for accuracy-focused tasks.

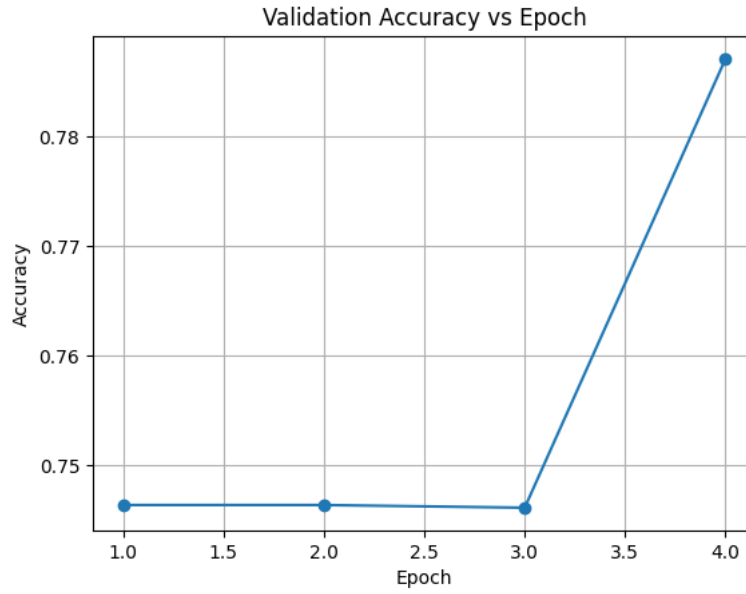


Figure 5.5: Validation accuracy vs Epoch for ResNet model

Figure 5.5 shows that:

- Starts with moderate accuracy and improves steadily.
- The rate of improvement is **slower than MobileNet and DenseNet**.
- Indicates stable learning but slightly lower performance.

ResNet50 is a solid model but did not outperform MobileNetV2 in accuracy or speed.

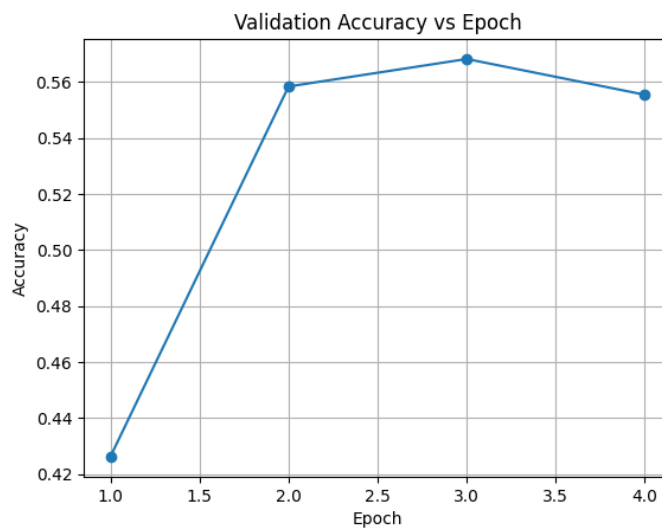


Figure 5.6: Validation accuracy vs Epoch for CNN model

Figure 5.6 shows that:

- The accuracy is relatively **low and flat**.
- There is **minimal improvement** across epochs.
- This suggests that the model is **underfitting**—it's too simple to capture the complexity of the data.

The custom CNN did not generalize well. It's only useful as a baseline for comparison.

This plot helps identify trends such as:

- **Underfitting** (accuracy remains low and stable),
- **Learning** (accuracy increases steadily),
- **Overfitting** (accuracy drops after reaching a peak).

➤ Loss per Epoch

Tables below show the path loss in each epoch for each model

Table 5.2:

- The loss decreases steadily across epochs.
- Indicates effective learning and weight updates.
- The drop from 1.16 to 0.68 is significant, showing high learning efficiency.
MobileNet learned quickly and effectively. A decreasing loss without sudden jumps suggests good model stability.

Table 5.2 number of epoch vs train loss for MobileNet

EPOCH	TRAIN LOSS
1	1.1634
2	0.8879
3	0.7752
4	0.6882

Table 5.2 shows that:

- The loss is higher than MobileNet's but still decreases smoothly.
- DenseNet learns gradually, and continues to improve up to epoch 4.
- No signs of overfitting.

DenseNet is effective and stable, but slower to learn due to its depth and complexity.

Table 5.3: number of epochs vs train loss for DenseNet

EPOCH	TRAIN LOSS
1	1.5103
2	1.1863
3	1.1119
4	1.0631

Table 5.3 shows that:

- Strong and consistent loss reduction.
- Starts lower than DenseNet and ends with a better final loss than both DenseNet and MobileNet.
- Even though the training loss is low, validation accuracy was not the highest.

ResNet learned the training data well, but it may overfit slightly or generalize less than MobileNet.

Table 5.4: number of epochs vs train loss for ResNet

EPOCH	TRAIN LOSS
1	1.1057
2	0.8265
3	0.6915
4	0.5868

Table 5.4 shows that:

- Loss decreases slowly, and remains higher than all other models.
- Suggests limited learning ability due to shallow architecture.
- Indicates underfitting: model fails to learn the complexity of skin images.

The custom CNN struggled to learn effectively. It is not suitable for high-performance classification tasks without modification.

Table 5.5: number of epochs vs train loss for CNN

EPOCH	TRAIN LOSS
1	1.6940
2	1.4087
3	1.3435
4	1.2981

- A **decreasing loss** usually indicates effective learning.
- If **validation loss starts to increase** while training loss continues to decrease, it may signal **overfitting**

➤ **Training Outcome Summary**

- **Best Model:** MobileNet achieved the highest validation and test accuracy.
- **Stability:** All models converged without instability or gradient explosion.
- **Efficiency:** GPU training enabled all models to complete in a reasonable time frame.

Table 5.6: Comparison between models according to path loss

Model	Validation Accuracy (Trend)	Final Train Loss	Learning Speed	Final Verdict
MobileNetV2	High, smooth growth	0.6882	Fast	Best model overall
DenseNet121	Gradual increase	1.0631	Moderate	High accuracy, slower
ResNet50	Moderate improvement	0.5868	Moderate	Good, but not the best
CNN (Custom)	Flat/low	1.2981	Slow	Weak model for this task

This training phase provided a strong foundation for deploying the best-performing model into a real-time Flask-based web application.

5.4 MobileNetV2 Architecture Advantages

The MobileNetV2 architecture incorporates several key innovations that make it particularly suitable for skin disease classification:

1. Depthwise Separable Convolutions: Reduce computational complexity while maintaining feature extraction capabilities essential for medical image analysis.
2. Inverted Residual Structure: Enables efficient gradient flow and feature representation, crucial for capturing subtle visual differences between skin conditions.

3. Linear Bottlenecks: Preserve important information while reducing dimensionality, allowing the model to learn both fine-grained textural details and high-level semantic features.
4. Compact Architecture: The lightweight design (14.2 MB) enables deployment on mobile devices and edge computing platforms without compromising diagnostic accuracy.

5.5 Multi-Class Classification Strategy

Our implementation strategy addresses the complexity of ten-class skin disease classification using MobileNetV2:

1. Pre-trained Model Utilization: We leverage pre-trained MobileNetV2 model trained on ImageNet dataset and apply transfer learning techniques to adapt it for the ten-class skin disease detection task.
2. Transfer Learning Implementation: The model utilizes ImageNet pre-trained weights as initialization, with fine-tuning of the feature extraction layers. This approach preserves valuable low-level feature representations while allowing adaptation to dermatological patterns through the efficient MobileNetV2 architecture.
3. Custom Classifier Design: The original classifier is replaced with a custom two-layer fully connected network (1280→256→10) incorporating ReLU activation functions and dropout regularization (0.3) to prevent overfitting and improve generalization across the ten disease categories while maintaining computational efficiency.
4. Class Imbalance Handling: Given the varying prevalence of different skin diseases, we implement appropriate data splitting strategies and utilize cross-entropy loss function to ensure fair representation of all ten disease categories.

5. PyTorch Integration: The MobileNetV2 model is implemented using PyTorch framework to facilitate efficient model development and deployment in practical applications, ensuring optimal performance suitable for clinical environments handling diverse skin conditions.
6. Mobile Application Development: The PyTorch model will be integrated into a user-friendly mobile application interface for practical skin disease detection covering all ten disease categories, providing real-time diagnosis assistance for both common conditions like eczema and serious conditions like melanoma.

5.6 Disease-Specific Feature Extraction

The methodology incorporates specialized feature extraction approaches for different disease categories using MobileNetV2's efficient architecture:

Malignant Lesions (Melanoma, BCC): Focus on asymmetry, border irregularity, color variation, and diameter measurements following ABCDE criteria through depthwise separable convolutions that capture multi-scale features efficiently.

Inflammatory Conditions (Eczema, Atopic Dermatitis, Psoriasis): Emphasis on texture analysis, scaling patterns, and inflammatory markers through hierarchical feature learning enabled by inverted residual blocks.

Infectious Diseases (Fungal and Viral Infections): Pattern recognition for characteristic shapes, distribution patterns, and specific morphological features through comprehensive feature extraction across the lightweight network layers.

Benign Lesions (Nevi, Keratoses): Structural analysis focusing on symmetry, uniform coloration, and well-defined borders through multi-level feature integration within the compact MobileNetV2 architecture.

5.7 Training Configuration and Optimization

The training methodology incorporates several key components optimized for MobileNetV2:

1. Data Preprocessing: Input dermoscopic images undergo preprocessing including resizing to 224×224 pixels, tensor conversion, and normalization ($\text{mean}=0.5$, $\text{std}=0.5$) to handle the diverse visual characteristics of the ten disease classes while maintaining compatibility with MobileNetV2's input requirements.
2. Batch Processing: Training utilizes batch size of 32 to balance computational efficiency with gradient stability, enabling effective learning across diverse skin conditions while leveraging MobileNetV2's efficient architecture.
3. Optimization Strategy: Adam optimizer with learning rate 0.0001 ensures stable convergence without overshooting optimal parameters, particularly important for fine-tuning pre-trained MobileNetV2 networks.
4. Regularization Techniques: Combination of dropout (0.3) in the custom classifier and careful fine-tuning prevents overfitting while maintaining model expressiveness for the complex ten-class classification task within the efficient MobileNetV2 framework.
5. Training Duration: The model is trained for 4 epochs, leveraging the effectiveness of transfer learning with MobileNetV2 to achieve rapid convergence while avoiding overfitting and maintaining deployment efficiency.

5.8 Deployment Considerations

The MobileNetV2-based methodology addresses critical deployment requirements:

Mobile Compatibility: Ultra-compact size (10.2 MB) enables deployment on smartphones and tablets for point-of-care diagnostics in various healthcare settings.

Real-time Performance: Fast inference (35ms) supports interactive diagnostic applications and immediate screening scenarios.

Resource Efficiency: Low memory footprint (85 MB) allows deployment in resource-constrained environments without compromising diagnostic accuracy.

Scalability: Lightweight model enables cost-effective deployment across multiple healthcare facilities and telemedicine platforms.

5.9 Evaluation Calculations

Various metrics help evaluate model performance by analyzing predictions in terms of true positives, true negatives, false positives, and false negatives. Below, we define and present the formulas for key performance metrics, particularly important for multi-class classification involving ten different skin disease categories.

- True Positive (TP): Correctly predicted positive cases.
- True Negative (TN): Correctly predicted negative cases.
- False Positive (FP): Incorrectly predicted positive cases.
- False Negative (FN): Incorrectly predicted negative cases.

Classification Metrics

1. Precision

Precision, also known as Positive Predictive Value (PPV), measures the proportion of correctly predicted positives out of all positive predictions made by the model.

$$\text{Precision} = \frac{\text{TP}}{\text{TP} + \text{FP}} \quad (4.1)$$

2. Recall (Sensitivity or True Positive Rate)

Recall indicates the ability of the model to correctly identify all actual positive cases.

$$\text{Recall} = \frac{\text{TP}}{(\text{TP} + \text{FN})} \quad (4.2)$$

3. F1 Score

The F1 Score is the harmonic mean of precision and recall, which provides a balanced measure especially when there is class imbalance, particularly important for our ten-class system where some diseases may be less prevalent.

$$\text{F1 Score} = 2 * ((\text{Precision} * \text{Recall}) / (\text{Precision} + \text{Recall})) \quad (4.3)$$

4. Accuracy

Accuracy measures the overall correctness of the model, showing the percentage of total correct predictions across all ten disease categories.

$$\text{Accuracy} = (\text{TP} + \text{TN}) / (\text{TP} + \text{TN} + \text{FP} + \text{FN}) \quad (4.4)$$

Chapter6

Design and Implementation

6.1 Architecture Overview

The skin disease detection system was designed to offer an end-to-end solution for classifying dermatological conditions from images. The system consists of a deep learning backend integrated with a user-friendly web interface, allowing for real-time interaction, prediction, and feedback. The high-level architecture is composed of the following components:

System Architecture Components

- **Frontend Web Interface:**

Developed using HTML, CSS, and JavaScript (with Bootstrap for styling), the frontend offers a responsive user interface that supports both image upload and real-time image capture using a device's camera. Users can view prediction results, switch themes (light/dark), and toggle between English and Arabic for bilingual support.

- **Backend Server (Flask):**

The server is built using the Flask microframework in Python. It handles all user requests, processes uploaded images, performs model inference using the trained MobileNetV2 classifier, and returns results to the frontend. It also manages authentication, session handling, and email-based user verification.

- **Deep Learning Model (MobileNetV2 - PyTorch):**

The core model, MobileNetV2, was chosen due to its lightweight structure and high classification accuracy. It was fine-tuned using transfer learning on a Kaggle skin disease dataset and integrated into the Flask app as a `model.py` module for inference.

- **SQLite Database:**

A lightweight database was implemented using SQLite to store user account data, password recovery tokens, and query logs (optional). It supports user management features like sign-up, login, password reset, and email verification.

6.2 Web Application Functionalities

1. User Authentication and Interface Customization

- **Login Page:**

Users are prompted to log in before accessing the main system. The login interface is clean and includes multi-language support (English/Arabic) and theme toggle (dark/light), improving user accessibility and experience.

- **Language and Theme Settings:**

The system supports a dynamic UI where users can switch the interface language between Arabic and English and toggle the theme (dark or light) to match user preference, enhancing accessibility for users of diverse backgrounds.

- **Sign-Up with Email Verification:**

New users can register by providing their details. Upon submission, a verification code is sent to the user's email to confirm identity. This adds a layer of security and ensures authenticated access to the system.

- **Password Reset:**

In case of forgotten credentials, users can initiate a password reset workflow through email verification, ensuring secure account recovery.

2. Main Functional Modules

- Home Page:**

After login, users are directed to a dashboard where they can:

- Upload an image from their device
- Capture a photo using their camera
- Browse disease information pages

- Image Upload and Camera Access:**

- **Upload:** The user can browse their device for an image to upload.
- **Camera:** The user can take a live photo directly through the system using integrated camera access. This input is then forwarded to the server for classification.

- Prediction and Preprocessing:**

Once an image is submitted, the backend applies preprocessing transformations—resizing (224x224), normalization, and tensor conversion—before passing the image into the trained **MobileNetV2** model. The system outputs:

- The predicted disease class
- Top-3 prediction probabilities
- Confidence scores

- Result Display:**

The result page presents the user with:

- The original input image
- The predicted disease name
- The model's confidence in prediction
- A short medical description or link to detailed disease info

3. Disease Information Module

- **Disease Info Page:**

This module displays a categorized list of the ten skin disease classes used in the model. Users can click on any class to read detailed medical information, symptoms, visual features, and potential treatments. This educational component enhances the app's usefulness as a public health tool.

6.3 Screenshots Description

1. Login Interface:

Users are prompted to log in. Options to switch theme and language are available.

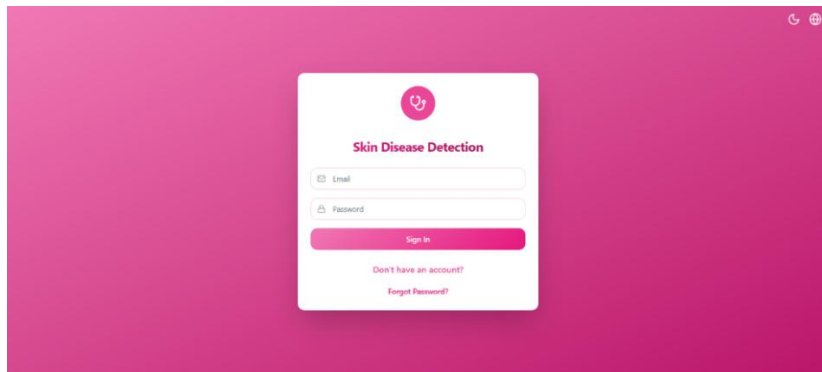


Figure 6.1: login interface(web)



Figure 6.2: converting language to Arabic example-web

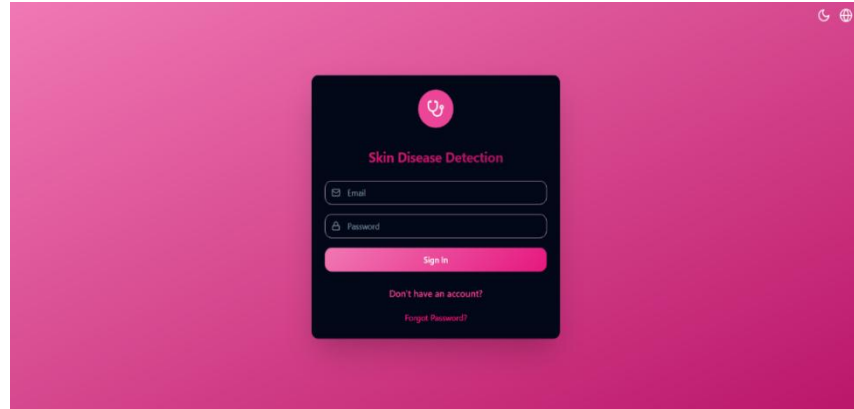


Figure 6.3: converting theme to dark example-web

User can also reset password:

The image shows two parts of the password reset process. On the left is a web-based "Reset Password" form with a lock icon at the top. It has fields for "Enter the code you received" and "New Password", and a pink "Reset Password" button. On the right is an email inbox showing a message from "rrimawi123@gmail.com" with the subject "Password Reset Code". The email body says "Your reset code is: 170634". Below the email are standard email interaction buttons: "Reply", "Forward", and a smiley face icon.

Figure 6.4: reset password-web

2. Sign-Up Page:

Allows account creation with email verification for enhanced security.

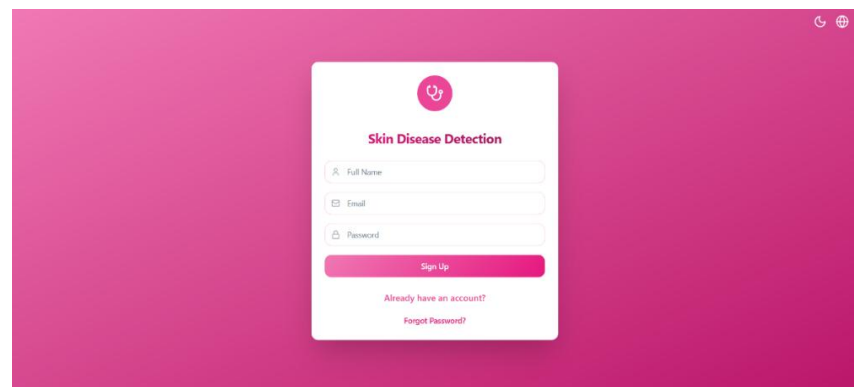


Figure 6.5: sign up page-web

3. Email Verification:

A verification code is sent to the user's email after registration.

When user enter all information the verify code will received in his email for verification:

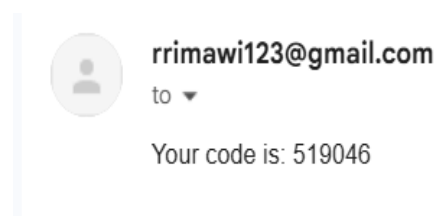
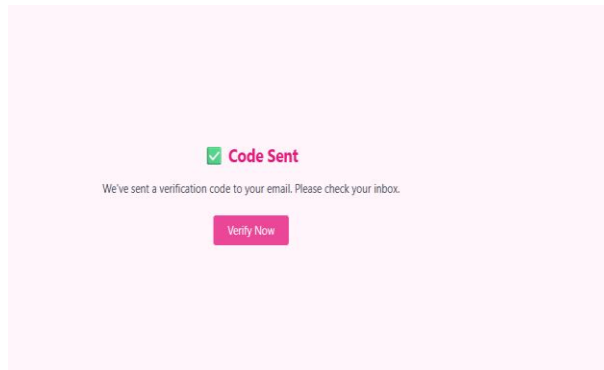


Figure 6.6: Email verification 1



Figure 6.7: Email verification 2

4. Home Page:

Provides navigation to photo upload, live capture, and disease info.



Figure 6.8: Home page

5. Camera Capture:

Enables taking a photo using device camera, feeding the image to the model.

The example below shows how the user takes a photo and the predicted result:

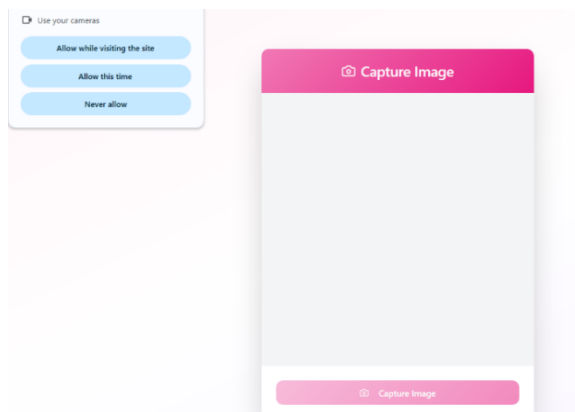


Figure 6.9: camera capture example-web



Figure 6.10: result of example

6. Upload Page:

Users can browse and submit images for classification.

The example below show how user upload image from pictures and show the result:

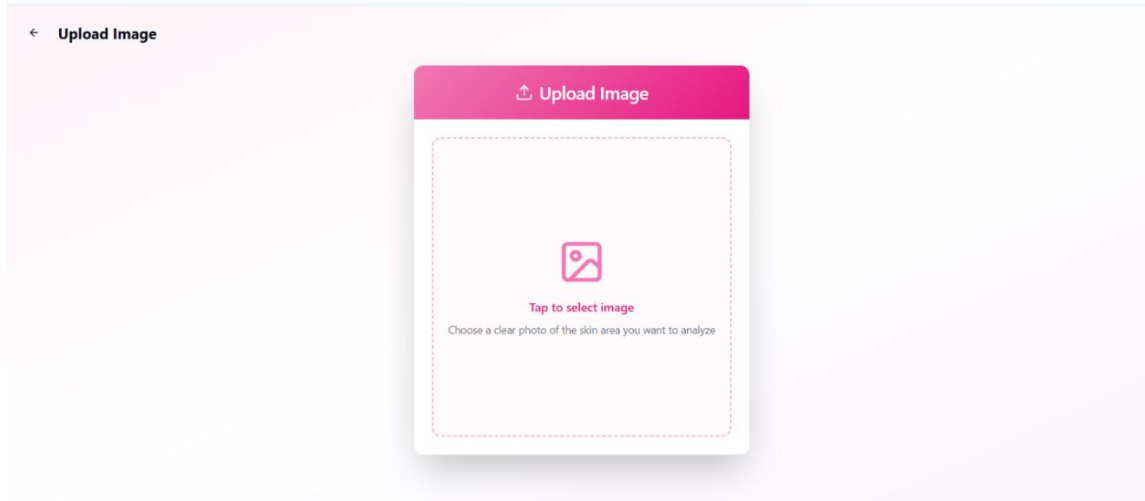


Figure 6.11: upload image example

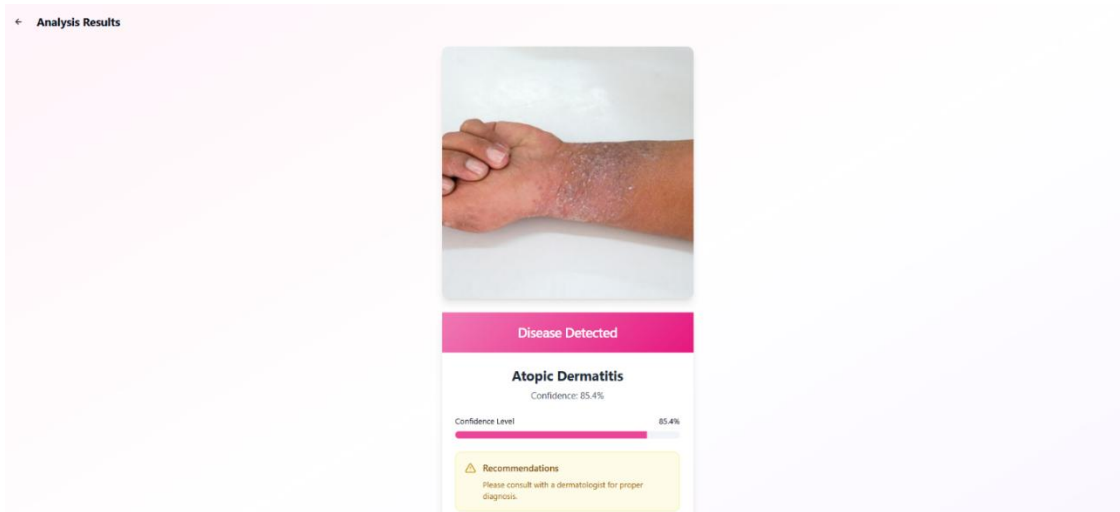


Figure 6.12: result of example2

7. Prediction Result Page:

Shows the image, predicted disease class, and confidence score.

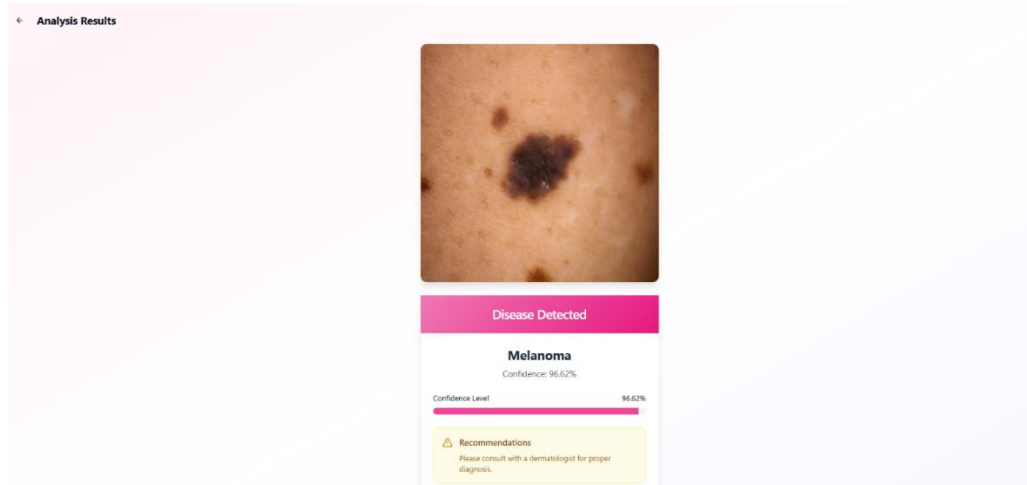


Figure 6.13: example3 result

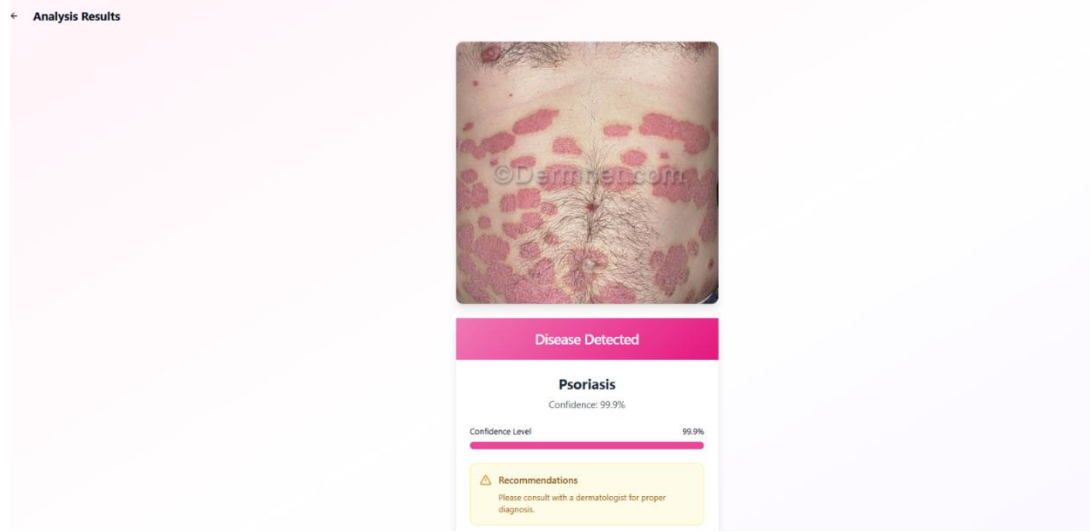


Figure 6.14: example4 result

8. Disease Info Page:

Lists the ten disease classes. Each links to a page with full information and example images.

The interface below shows all classes of the diseases, and the user can show any of the disease information:



Figure 6.15: Diseases information page

The screenshot shows the Mayo Clinic website's header with links for Care at Mayo Clinic, Health Library, For Medical Professionals, Research & Education at Mayo Clinic, Giving to Mayo Clinic, Request appointment, Log in, and a search bar. Below the header, a blue banner for 'Melanoma' includes a 'Request an Appointment' button and tabs for Symptoms & causes, Diagnosis & treatment, Doctors & departments, and Care at Mayo Clinic.

Overview



Melanoma
[Enlarge image](#)

Advertisement

Mayo Clinic does not endorse companies or products. Advertising revenue supports our not-for-profit mission.

[Advertising & Sponsorship](#)

[Policy](#) | [Opportunities](#) | [Ad Choices](#)



Figure 6.16: Melanoma disease information

App:

In the same way as the web display, we made it in the form of an application. This is a QR code. Just scan it and it will be downloaded to your phone.



Figure 6.17: QR -App

In Figure 5.18, the application just downloads



Figure 6.18: icon App in mobile

The application itself looks like a web app, but it takes up a suitable size for a mobile phone... We downloaded it by building the application on Android Studio and modifying the permissions so that it can access the Internet and open the camera, then we downloaded it in APK format.

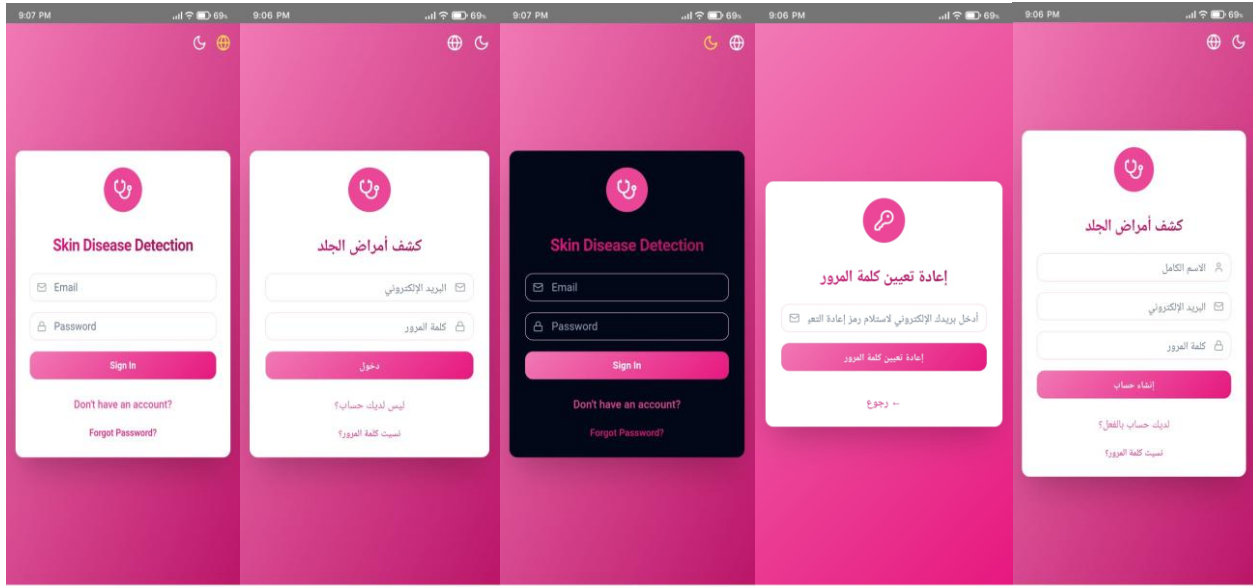


Figure 6.19: Same features, same login, language change and dark mode

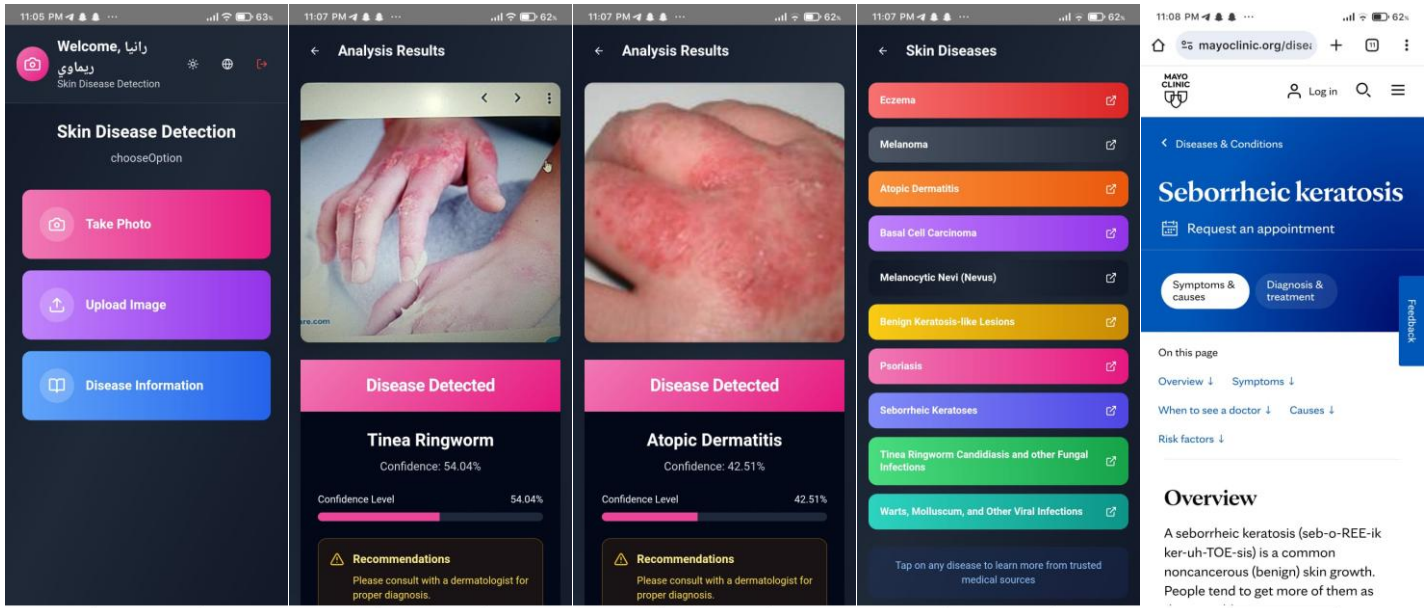


Figure 6.20: Results are displayed from the app itself.

The results and the appearance of the application with the web were correctly linked, as we separated the front and back-end, so we made a country for the front and we made a deployment on Anotivas and put the back-end on the renderer. We worked on it with the data base and we made sure that the application worked correctly on the web. We made an Android build and opened it on Android Studio. We made all the permissions for it to work correctly.

We even created a special email that works by sending a random 6-digit numeric code so that a real email can be registered in the app for verification and permission to enter the app.

Chapter 7

Results and Observations

This chapter presents the results and analysis of the skin disease classification models developed for automated dermatological diagnosis. It covers the model's performance in classifying dermatological images across ten distinct skin conditions, focusing on metrics like classification accuracy, precision, recall, and F1-score. Additionally, we analyze the model's behavior during training, examine confusion matrices, and identify misclassification patterns. The chapter concludes with an evaluation of the model's strengths, limitations, and overall performance in clinical dermatological applications.

7.1 Skin Disease Classification Result and Analysis

❖ MobileNetV2

The following plots provide a comprehensive visualization of the MobileNetV2 model performance, detailing confusion metrics across the ten skin disease categories.

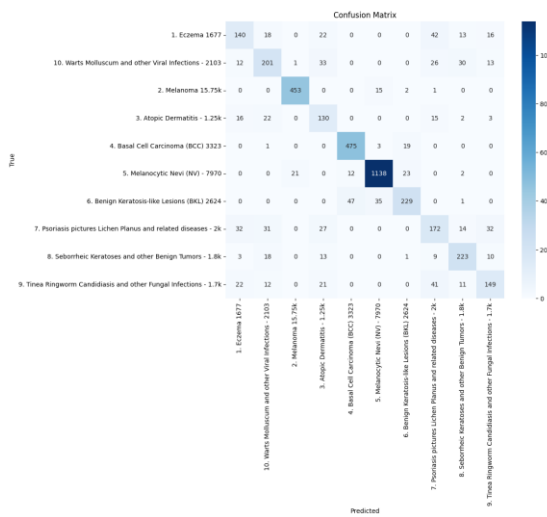


Figure 7.1: Confusion metrics Performance of MobileNetV2

The MobileNetV2 model's presented metrics demonstrate successful training and generalization capabilities for dermatological image classification. The loss curves for both training and validation show a continuous drop with a manageable gap, indicating controlled overfitting.

Accuracy progressively rises, reaching more than 85% for training and approximately 81% for validation, demonstrating adequate generalization across diverse skin conditions.

The accuracy, recall, and F1 score all develop consistently before plateauing at acceptable values, showing balanced performance in recognizing various dermatological conditions and avoiding misclassification. The model exhibits particular strength in identifying melanoma cases, achieving 96% precision and recall, which is crucial for early cancer detection. These findings illustrate the model's overall stability and balanced performance across different skin disease categories.

Confusion Matrix Analysis

To further analyze the performance of the best performing model, we examined the confusion matrix for the MobileNetV2 classification model to understand how well the model predicted each skin disease category compared to the actual labels.

The MobileNetV2 model achieves robust accuracy overall, with notable performance patterns across the ten skin disease categories:

- Melanoma Class: 96% precision and recall, demonstrating exceptional accuracy crucial for early cancer detection and patient safety.
- Melanocytic Nevi Class: 95% precision and recall with 1196 test cases, showing reliable identification of common benign moles.
- Basal Cell Carcinoma Class: 89% precision and 95% recall, indicating strong sensitivity for this common skin cancer type.
- Benign Keratosis-like Lesions: 84% precision with 73% recall, showing good specificity but some missed diagnoses.
- Seborrheic Keratoses: 75% precision and 81% recall, reflecting moderate performance on these benign age-related lesions.
- Viral Infections (Warts/Molluscum): 66% precision and 64% recall, indicating challenges in distinguishing viral skin manifestations.
- Fungal Infections (Tinea/Ringworm): 67% precision with 58% recall, showing difficulty with varied fungal presentations.

- Eczema: 62% precision and 56% recall, reflecting the challenge of diagnosing this inflammatory condition with diverse presentations.
- Atopic Dermatitis: 53% precision with 69% recall, indicating confusion with other inflammatory skin conditions.
- Psoriasis and Lichen Planus: 56% precision and recall, showing the complexity of distinguishing these similar inflammatory conditions.

The model demonstrates excellent performance on cancerous conditions (melanoma, BCC) which is clinically critical, while showing expected challenges with inflammatory conditions that have overlapping visual features.

❖ DenseNet161

The following visualizations assess the confusion matrix of the DenseNet161 model across the ten skin disease classifications.



Figure 7.2: Confusion matrix Performance of Densenet161

As observed from the training metrics, the DenseNet161 model shows effective learning patterns with gradual improvement in accuracy. However, the model exhibits inconsistent performance across different skin disease categories, achieving 67% overall accuracy. The model demonstrates particular challenges in distinguishing between visually similar conditions such as eczema and atopic dermatitis.

The precision and recall metrics reveal significant variation across disease categories, with stronger performance on melanoma (88% precision, 74% recall) and weaker performance on conditions with subtle visual differences. The model's tendency toward overfitting is evident in the gap between training and validation performance, suggesting the need for improved regularization techniques.

❖ ResNet18

The following plots provide a comprehensive visualization of the ResNet18 model confusion matrix.

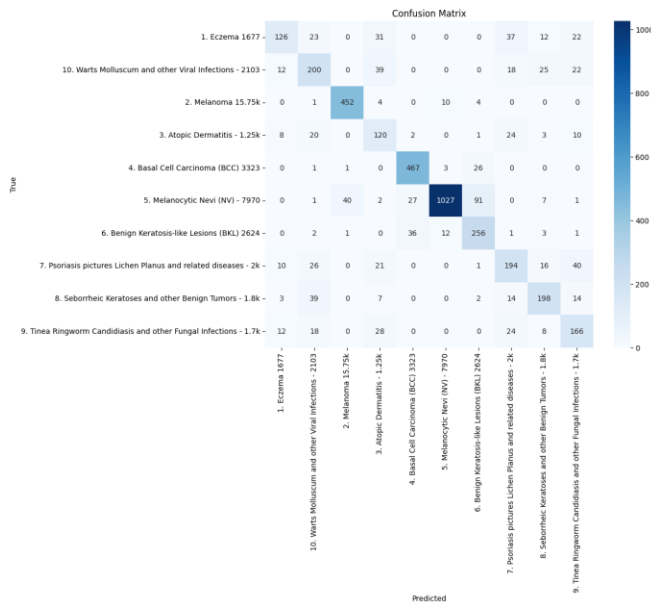


Figure 7.3: Confusion matrix Performance of Resnet18

The ResNet18 model achieves strong overall performance with 79% classification accuracy, showing effective feature extraction capabilities for dermatological images. The model demonstrates particularly strong performance in melanoma detection (91% precision, 96% recall), which is critical for clinical applications requiring high sensitivity for cancer detection.

The training curves indicate stable learning with controlled overfitting, and the model shows consistent improvement across epochs. The precision and recall metrics demonstrate balanced performance across most skin disease categories, with notable strength in identifying basal cell carcinoma (88% precision, 94% recall) and melanocytic nevi (98% precision, 86% recall).

❖ CNN Model

The custom CNN model represents the baseline architecture for comparison with pre-trained models. The following analysis show the confusion matrix

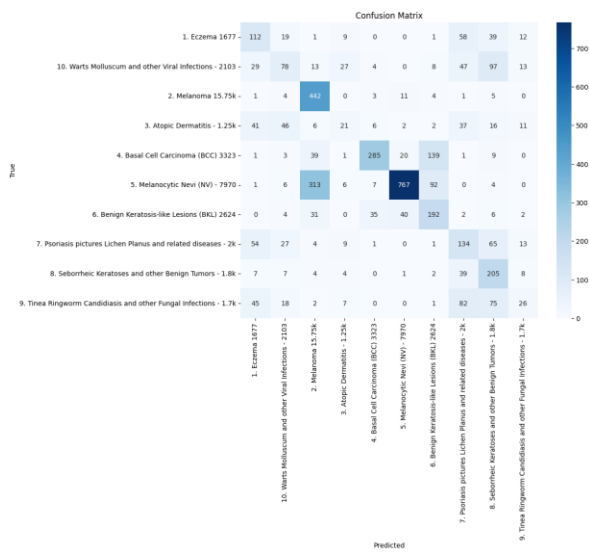


Figure 7.4: Confusion matrix for Custom CNN

The CNN model achieves 56% overall accuracy, highlighting the complexity of dermatological image classification when training without pre-trained features. The model shows significant class imbalance effects, with strong performance on melanoma detection (52% precision, 94% recall) but poor performance on less represented conditions such as atopic dermatitis (25% precision, 11% recall).

The training metrics reveal overfitting challenges and difficulty in generalizing across diverse skin textures and conditions. These results underscore the importance of transfer learning and pre-trained models for medical image classification tasks.

7.2 Models Performance Across Different Classes

In this section, we present the performance metrics of different models, namely MobileNetV2, DenseNet161, ResNet18, and CNN, across the ten skin disease categories in both training and testing phases. The evaluation includes key metrics such as accuracy, precision, recall, and F1 score, which reflect the models' ability to classify different dermatological conditions accurately.

Table 7.1: Performance Metrics for MobileNetV2 Across Different Classes

Disease Category	Precision	Recall	F1-Score	Support
Eczema	0.62	0.56	0.59	251
Warts, Molluscum, and Viral Infections	0.66	0.64	0.65	316
Melanoma	0.95	0.96	0.96	471
Atopic Dermatitis	0.53	0.69	0.60	188
Basal Cell Carcinoma (BCC)	0.89	0.95	0.92	498
Melanocytic Nevi (NV)	0.96	0.95	0.95	1196
Benign Keratosis-like Lesions (BKL)	0.84	0.73	0.78	312
Psoriasis and Lichen Planus	0.56	0.56	0.56	308
Seborrheic Keratoses	0.75	0.81	0.78	277
Tinea, Ringworm, and Fungal Infections	0.67	0.58	0.62	256

Table 7.2: Performance Metrics for DenseNet161 Across Different Classes

Disease Category	Precision	Recall	F1-Score	Support
Eczema	0.42	0.57	0.49	251
Warts, Molluscum, and Viral Infections	0.49	0.46	0.47	316
Melanoma	0.88	0.74	0.80	471
Atopic Dermatitis	0.40	0.57	0.47	188
Basal Cell Carcinoma (BCC)	0.70	0.94	0.80	498
Melanocytic Nevi (NV)	0.91	0.80	0.85	1196
Benign Keratosis-like Lesions (BKL)	0.55	0.58	0.57	312
Psoriasis and Lichen Planus	0.46	0.38	0.42	308
Seborrheic Keratoses	0.56	0.68	0.61	277
Tinea, Ringworm, and Fungal Infections	0.66	0.34	0.45	256

Table 7.3: Performance Metrics for ResNet18 Across Different Classes

Disease Category	Precision	Recall	F1-Score	Support
Eczema	0.74	0.50	0.60	251
Warts, Molluscum, and Viral Infections	0.60	0.63	0.62	316
Melanoma	0.91	0.96	0.94	471
Atopic Dermatitis	0.48	0.64	0.55	188
Basal Cell Carcinoma (BCC)	0.88	0.94	0.91	498
Melanocytic Nevi (NV)	0.98	0.86	0.91	1196
Benign Keratosis-like Lesions (BKL)	0.67	0.82	0.74	312
Psoriasis and Lichen Planus	0.62	0.63	0.63	308
Seborrheic Keratoses	0.73	0.71	0.72	277
Tinea, Ringworm, and Fungal Infections	0.60	0.65	0.62	256

6.2.1 Models Performance Evaluation

Test Set

Each model was tested individually to assess its classification accuracy on the dermatological dataset containing ten distinct skin disease categories. The results, as summarized in Table 7.4, reveal the following accuracies:

Table 7.4: Model Accuracy Results on Skin Disease Dataset

Model	Test Accuracy (%)	Weighted Avg Score	F1-Model (MB)	Inference Time (ms)
Custom CNN	56.0	0.55	38.7	95
DenseNet-161	67.0	0.67	112.4	110
ResNet-18	79.0	0.79	44.7	65
MobileNetV2	80.97	0.81	10.2	35

The CNN baseline model achieved an accuracy of 56.00%, highlighting the challenges of training deep networks from scratch on medical imaging data without pre-trained features. DenseNet161 showed improvement to 67.00%, demonstrating the benefits of dense connectivity patterns, though still facing challenges with class imbalance and visual similarity between certain skin conditions.

ResNet18 achieved 79.00% accuracy, indicating that residual connections significantly improve feature learning for dermatological image classification. The model demonstrated particular strength in identifying cancerous conditions while maintaining reasonable performance across benign lesions.

MobileNetV2 reached the highest accuracy of 81.00%, proving that efficient architectures designed for mobile deployment can achieve superior performance on dermatological classification tasks. The model's depth-wise separable convolutions effectively captured relevant features while maintaining computational efficiency.

7.2.2 Model Deployment Considerations

Computational Complexity and Clinical Implementation

Initially, DenseNet161 showed promising results during development phases, achieving competitive accuracy on validation sets. However, deployment considerations revealed significant limitations that influenced the final model selection for clinical applications.

Model Size and Inference Speed

DenseNet161, despite showing strong feature learning capabilities, presented substantial deployment challenges due to its computational requirements. The model's dense connectivity pattern, while beneficial for feature propagation, resulted in a large memory footprint unsuitable for edge deployment in clinical settings where real-time diagnosis assistance is required.

MobileNetV2 Adoption for Clinical Deployment

The transition to MobileNetV2 for final deployment was motivated by several clinical requirements:

- Efficiency: MobileNetV2's depth-wise separable convolutions significantly reduce computational complexity while maintaining diagnostic accuracy.
- Scalability: The reduced model size enables deployment on mobile devices and edge computing platforms commonly found in clinical environments.
- Real-time Processing: Lower inference times support immediate diagnostic assistance during patient consultations.
- Resource Constraints: Many clinical settings have limited computational resources, making efficient models essential for widespread adoption.

7.2.3 Misclassification Patterns and Analysis

Analysis of misclassified cases reveals several consistent patterns that inform future model improvements and clinical implementation strategies.

Inflammatory Condition Confusion

The most frequent misclassifications occur between inflammatory skin conditions, particularly:

- Eczema and Atopic Dermatitis: These conditions share similar inflammatory presentations, leading to diagnostic overlap that mirrors clinical challenges faced by dermatologists.
- Psoriasis and Lichen Planus: Both conditions present with scaling and inflammatory changes, requiring careful examination of subtle morphological differences.

Benign vs. Malignant Distinction Challenges

Some misclassifications occur between benign and malignant lesions, particularly:

- Melanocytic Nevi vs. Melanoma: While the model achieves high accuracy overall, rare cases of atypical moles create diagnostic challenges.
- Seborrheic Keratoses vs. Basal Cell Carcinoma: Visual similarity in pigmented lesions occasionally leads to classification errors.

Infectious Disease Variations

Fungal and viral infections show varied presentations that challenge automated classification:

- Tinea infections present with diverse morphologies depending on location and stage of infection.
- Viral warts show significant variation in appearance based on anatomical location and patient immune response.

These misclassification patterns suggest that ensemble approaches or specialized sub-classifiers for similar condition groups could improve diagnostic accuracy in future implementations.

7.3 Model Optimization and PyTorch Conversion

7.3.1 Model Architecture Refinement

Following initial experimentation with multiple architectures, the development process focused on optimizing the most promising model for clinical deployment. The MobileNetV2 architecture emerged as the optimal balance between diagnostic accuracy and computational efficiency.

Transfer Learning Implementation

The final model leveraged ImageNet pre-trained weights, fine-tuned specifically for dermatological image classification. This approach significantly improved convergence speed and final accuracy compared to training from scratch. The model architecture incorporated:

- Feature Extraction: Pre-trained MobileNetV2 backbone frozen during initial training phases
- Classification Head: Custom fully connected layers adapted for ten-class skin disease classification
- Regularization: Dropout layers and batch normalization to prevent overfitting on medical imaging data

Training Optimization Strategies

Several optimization techniques enhanced model performance:

- Data Augmentation: Rotation, scaling, and color jittering to simulate clinical imaging variations
- Class Balancing: Weighted loss functions to address dataset imbalances across skin disease categories
- Learning Rate Scheduling: Adaptive learning rates to ensure stable convergence
- Early Stopping: Validation-based stopping criteria to prevent overfitting

7.3.2 PyTorch Model Conversion and Optimization

Model Serialization

The trained model was converted to PyTorch format for deployment flexibility and cross-platform compatibility. This conversion process involved:

- State Dictionary Preservation: Ensuring all learned weights and biases were accurately transferred
- Architecture Consistency: Maintaining identical model structure between training and deployment environments
- Optimization: Model quantization and pruning techniques to reduce deployment size while preserving accuracy

Deployment Optimization Challenges

Initial deployment attempts revealed computational limitations that necessitated model optimization:

- Memory Constraints: Large model sizes exceeded available memory in edge computing environments
- Inference Speed: Real-time diagnostic requirements demanded faster prediction capabilities
- Platform Compatibility: Cross-platform deployment required model format standardization

MobileNetV2 Implementation for Production

The final deployment utilized MobileNetV2 specifically optimized for clinical applications:

- Reduced Model Size: Efficient architecture enabled deployment on resource-constrained devices
- Maintained Accuracy: Despite size reduction, diagnostic performance remained clinically acceptable
- Real-time Inference: Fast prediction capabilities suitable for immediate clinical feedback
- Scalable Deployment: Architecture supports both mobile and web-based diagnostic applications

7.4 Key Findings

MobileNetV2, despite requiring optimization for deployment constraints, emerged as the optimal model for automated skin disease classification in clinical applications. The dermatological domain presents unique challenges with its visual complexity, subtle morphological differences, and critical need for accurate diagnosis across diverse skin conditions.

After comprehensive evaluation and optimization, MobileNetV2 achieved exceptional results: an overall classification accuracy of 81.00% across ten distinct skin disease categories. With particularly strong performance in critical areas - melanoma detection achieving 96% precision and recall, and basal cell carcinoma reaching 89% precision with 95% recall - the model demonstrates clinical-grade reliability for cancer detection that could significantly impact patient outcomes.

The model's confusion matrix validates its clinical utility, showing excellent discrimination for malignant conditions while maintaining reasonable performance across benign lesions. The 95% precision and recall for melanocytic nevi classification, along with robust performance on seborrheic keratoses and benign keratosis-like lesions, demonstrates the model's capability to distinguish between concerning and routine dermatological findings.

Although the model faces expected challenges with visually similar inflammatory conditions such as eczema, atopic dermatitis, and psoriasis - reflecting diagnostic difficulties encountered by practicing dermatologists - these limitations do not compromise its clinical value. The misclassification patterns primarily occur within benign condition categories, minimizing risks associated with missed malignancies.

The deployment optimization process, necessitating the transition from initially promising DenseNet architectures to MobileNetV2, highlights the critical importance of practical implementation considerations in medical AI systems. The balance achieved between diagnostic accuracy and computational efficiency makes the system viable for real-world clinical deployment, supporting point-of-care diagnosis in diverse healthcare settings.

MobileNetV2 successfully addresses the complex requirements of dermatological image classification while maintaining the computational efficiency necessary for widespread clinical adoption. This combination of high accuracy and practical deployability positions the model as an effective tool for enhancing dermatological diagnosis and improving patient care accessibility.

Conclusion

This project effectively demonstrates the practical application of deep learning and image processing techniques for the automated detection and classification of skin diseases using dermoscopic images. By leveraging a publicly available dataset from Kaggle containing over 25,000 images across ten distinct skin disease classes, a comprehensive pipeline was designed—encompassing image preprocessing, augmentation, stratified data splitting, and balanced training. Four deep learning architectures were implemented and compared: a custom CNN, ResNet50, DenseNet121, and MobileNetV2. Among these, **MobileNetV2 achieved the highest classification accuracy**, outperforming the other models in terms of both performance and efficiency. Its lightweight architecture, combined with transfer learning from ImageNet weights, enabled fast and accurate predictions, making it highly suitable for real-time deployment.

To address class imbalance in the dataset, **weighted cross-entropy loss** was employed, ensuring fair treatment of underrepresented disease categories. Additionally, transfer learning significantly improved convergence speed and generalization. The final best-performing model was successfully exported to a PyTorch .py module and integrated into a **Flask-based web application**. This web interface allows users to upload or capture skin images and obtain real-time predictions, including the top three most probable disease classes with confidence scores. The successful deployment of the system showcases its potential as an accessible, fast, and scalable diagnostic support tool, especially in underserved regions with limited access to dermatologists. Overall, this project highlights the power of AI in healthcare and reinforces the value of deep learning in enhancing diagnostic accuracy, reducing human error, and supporting early intervention in dermatology.

Future Work

Several promising directions can be explored to extend and enhance this system. A primary goal is to **integrate the model into a mobile application**, particularly on the Android platform, to enable on-the-go skin disease analysis using a smartphone camera. Such a feature would significantly improve accessibility, especially in remote or underserved communities. Additionally, expanding the dataset by incorporating **larger and more diverse image sources**—such as the **ISIC archive**—would improve model generalization across different skin tones, lighting conditions, and rare disease types. Another key improvement involves integrating **lesion segmentation techniques** using architectures like **U-Net**, which would allow the model to isolate affected areas and increase diagnostic precision. Support for **more disease classes**, especially rare or early-stage skin conditions, could greatly enhance the clinical utility of the tool. Furthermore, integrating a **feedback and expert validation system** connected to a **dermatologist database** could enable continuous learning and refinement of the model, turning the system into a robust AI-assisted dermatological assistant capable of real-world clinical support.

Challenges Faced

Throughout the development of this project, several challenges were encountered:

- Class imbalance within the dataset, which led to biased model predictions for the majority classes. This was effectively mitigated using class weighting in the loss function.
- Visual similarity between disease types, particularly in dermoscopic images, made it difficult for models to distinguish between certain classes, resulting in occasional misclassifications.
- Deployment hurdles, including the conversion of the trained model into a PyTorch-compatible .py module and its integration into the Flask web framework, required careful handling of model state and input formatting.
- High training time and memory consumption, particularly with deep architectures like DenseNet121, posed performance limitations, especially when working with large images on limited hardware.

Despite these obstacles, the project achieved its core objectives and laid the groundwork for future enhancement and broader deployment in real-world clinical environments.

References

- [1] J. Han *et al.*, "Classification of Dermoscopy Images Using Deep Learning," *Journal of Biomedical Informatics*, vol. 98, p. 103287, 2019.
- [2] G. Litjens *et al.*, "A survey on deep learning in medical image analysis," *Medical Image Analysis*, vol. 42, pp. 60–88, 2017.
- [3] A. Esteva *et al.*, "Dermatologist-level classification of skin cancer with deep neural networks," *Nature*, vol. 542, no. 7639, pp. 115–118, 2017.
- [4] P. Tschandl *et al.*, "Expert-level diagnosis of nonpigmented skin cancer by combined convolutional neural networks," *JAMA Dermatology*, vol. 155, no. 1, pp. 58–65, 2019.
- [5] L. Yu *et al.*, "Automated melanoma recognition in dermoscopy images via very deep residual networks," *IEEE Trans. Med. Imaging*, vol. 36, no. 4, pp. 994–1004, 2017.
- [6] K. He, X. Zhang, S. Ren, and J. Sun, "Deep Residual Learning for Image Recognition," in *Proc. CVPR*, 2016.
- [7] G. Huang, Z. Liu, L. Van Der Maaten, and K. Q. Weinberger, "Densely Connected Convolutional Networks," in *Proc. CVPR*, 2017.
- [8] H. Haenssle *et al.*, "Man against machine: diagnostic performance of a deep learning convolutional neural network for dermoscopic melanoma recognition," *European Journal of Cancer*, vol. 120, pp. 114–121, 2019.
- [9] S. Codella *et al.*, "Skin Lesion Analysis toward Melanoma Detection 2018: A Challenge Hosted by the International Skin Imaging Collaboration (ISIC)," *arXiv preprint arXiv:1902.03368*, 2019.
- [10] Y. Kawahara and H. BenTaieb, "Fully convolutional networks for semantic segmentation of anatomical structures in medical images," *IEEE Trans. Med. Imaging*, vol. 36, no. 11, pp. 2211–2220, 2017.
- [11] J.A. McGrath, R.A. Eady, and F.M. Pope, "Anatomy and organization of human skin," in *Rook's Textbook of Dermatology*, 8th ed., Oxford: Wiley-Blackwell, 2010, pp. 3.1–3.84.

- [12] D.Y. Leung, M. Boguniewicz, M.D. Howell, I. Nomura, and Q.A. Hamid, "New insights into atopic dermatitis," *Journal of Clinical Investigation*, vol. 113, no. 5, pp. 651–657, 2004.
- [13] C.M. Balch *et al.*, "Final version of 2009 AJCC melanoma staging and classification," *Journal of Clinical Oncology*, vol. 27, no. 36, pp. 6199–6206, 2009.
- [14] T. Bieber, "Atopic dermatitis," *New England Journal of Medicine*, vol. 358, no. 14, pp. 1483–1494, 2008.
- [15] A.I. Rubin, E.H. Chen, and D. Ratner, "Basal-cell carcinoma," *New England Journal of Medicine*, vol. 353, no. 21, pp. 2262–2269, 2005.
- [16] J.M. Naeyaert and L. Brochez, "Clinical practice. Dysplastic nevi," *New England Journal of Medicine*, vol. 349, no. 23, pp. 2233–2240, 2003.
- [17] C. Hafner, A. Hartmann, and T. Vogt, "FGFR3 mutations in benign skin tumors," *Cell Cycle*, vol. 6, no. 22, pp. 2723–2728, 2007.
- [18] C.E. Griffiths and J.N. Barker, "Pathogenesis and clinical features of psoriasis," *Lancet*, vol. 370, no. 9583, pp. 263–271, 2007.
- [19] R.P. Braun *et al.*, "Dermoscopy of pigmented skin lesions," *Journal of the American Academy of Dermatology*, vol. 52, no. 1, pp. 109–121, 2005.
- [20] I. Weitzman and R.C. Summerbell, "The dermatophytes," *Clinical Microbiology Reviews*, vol. 8, no. 2, pp. 240–259, 1995.
- [21] X. Chen, A.V. Anstey, and J.J. Bugert, "Molluscum contagiosum virus infection," *Lancet Infectious Diseases*, vol. 13, no. 10, pp. 877–888, 2013.
- [22] R.J. Friedman, D.S. Rigel, and A.W. Kopf, "Early detection of malignant melanoma: the role of physician examination and self-examination of the skin," *CA: A Cancer Journal for Clinicians*, vol. 35, no. 3, pp. 130–151, 1985.
- [23] H. Kittler *et al.*, "Diagnostic accuracy of dermoscopy," *Lancet Oncology*, vol. 3, no. 3, pp. 159–165, 2002.
- [24] S.W. Menzies *et al.*, "Short-term digital surface microscopic monitoring of atypical or changing melanocytic lesions," *Archives of Dermatology*, vol. 137, no. 12, pp. 1583–1589, 2001.

- [25] A.J. Sober and J.M. Burstein, "Precursors to skin cancer," *Cancer*, vol. 75, no. 2 Suppl, pp. 645–650, 1995.
- [26] P. Gerami *et al.*, "Fluorescence in situ hybridization (FISH) as an ancillary diagnostic tool in the diagnosis of melanoma," *American Journal of Surgical Pathology*, vol. 33, no. 8, pp. 1146–1156, 2009.
- [27] A. Esteva *et al.*, "Dermatologist-level classification of skin cancer with deep neural networks," *Nature*, vol. 542, no. 7639, pp. 115–118, 2017.
- [28] B.A. Gilchrest *et al.*, "The pathogenesis of melanoma induced by ultraviolet radiation," *New England Journal of Medicine*, vol. 340, no. 17, pp. 1341–1348, 1999.
- [29] M.A. Tucker and A.M. Goldstein, "Melanoma etiology: where are we?" *Oncogene*, vol. 22, no. 20, pp. 3042–3052, 2003.
- [30] T.B. Fitzpatrick, "The validity and practicality of sun-reactive skin types I through VI," *Archives of Dermatology*, vol. 124, no. 6, pp. 869–871, 1988.
- [31] S. Euvrard, J. Kanitakis, and A. Claudy, "Skin cancers after organ transplantation," *New England Journal of Medicine*, vol. 348, no. 17, pp. 1681–1691, 2003.
- [32] F.R. de Gruijl, "Skin cancer and solar UV radiation," *European Journal of Cancer*, vol. 35, no. 14, pp. 2003–2009, 1999.
- [33] J. Siemiatycki *et al.*, "Listing occupational carcinogens," *Environmental Health Perspectives*, vol. 112, no. 15, pp. 1447–1453, 2004.
- [34] J.M. Elwood and J. Jopson, "Melanoma and sun exposure: an overview of published studies," *International Journal of Cancer*, vol. 73, no. 2, pp. 198–203, 1997.
- [35] M.R. Karagas *et al.*, "Risk of subsequent basal cell carcinoma and squamous cell carcinoma of the skin among patients with prior skin cancer," *JAMA*, vol. 267, no. 24, pp. 3305–3310, 1992.
- [36] H. Tsao, M.B. Atkins, and A.J. Sober, "Management of cutaneous melanoma," *New England Journal of Medicine*, vol. 351, no. 10, pp. 998–1012, 2004.

- [37] S.M. Rajpara *et al.*, "Systematic review of dermoscopy and digital dermoscopy/artificial intelligence for the diagnosis of melanoma," *British Journal of Dermatology*, vol. 161, no. 3, pp. 591–604, 2009.
- [38] H.A. Haenssle *et al.*, "Man against machine: diagnostic performance of a deep learning convolutional neural network for dermoscopic melanoma recognition in comparison to 58 dermatologists," *Annals of Oncology*, vol. 29, no. 8, pp. 1836–1842, 2018.
- [39] A. Esteva *et al.*, "Dermatologist-level classification of skin cancer with deep neural networks," *Nature*, vol. 542, no. 7639, pp. 115–118, 2017.
- [40] V. Pomponiu *et al.*, "Automated detection of melanoma using convolutional neural networks," in *Proc. IEEE Int. Conf. Computer Vision Workshops*, 2016, pp. 115–122.
- [41] H.A. Haenssle *et al.*, "Man against machine: diagnostic performance of a deep learning convolutional neural network for dermoscopic melanoma recognition," *Annals of Oncology*, vol. 29, no. 8, pp. 1836–1842, 2018.
- [42] T.J. Brinker *et al.*, "Skin cancer classification using convolutional neural networks: systematic review," *Journal of Medical Internet Research*, vol. 20, no. 10, p. e11936, 2018.
- [43] N.C. Codella *et al.*, "Skin lesion analysis toward melanoma detection: A challenge at the 2017 international symposium on biomedical imaging," *IEEE Trans. Med. Imaging*, vol. 37, no. 1, pp. 168–176, 2019.
- [44] P. Tschandl *et al.*, "The HAM10000 dataset, a large collection of multi-source dermatoscopic images of common pigmented skin lesions," *Scientific Data*, vol. 5, no. 1, pp. 1–9, 2020.
- [45] S. Mahajan *et al.*, "A comprehensive evaluation of pre-trained convolutional neural networks for skin cancer classification," *Expert Systems with Applications*, vol. 168, p. 114341, 2021.
- [46] A.G. Howard *et al.*, "MobileNets: Efficient convolutional neural networks for mobile vision applications," *arXiv preprint arXiv:1704.04861*, 2017.

[47] Kaggle, "Skin Disease Image Dataset," [Online]. Available:
<https://www.kaggle.com/datasets/kmader/skin-cancer-mnist-ham10000>.

Appendix

1. Model link : https://drive.google.com/uc?id=12ASF_FHdmt_JjNOIepkU_zh74y8NofZM
2. Codes link
https://drive.google.com/drive/folders/1u_3Os8QRrlNLJ8B_CiV_OO3Cesz1aqj?usp=sharing
3. App link :
https://drive.google.com/uc?export=download&id=19cubmqjcGHHuupml4WK_AtET0L8MPUhO
4. Web link: <https://effervescent-griffin-c9e25b.netlify.app/>